의학박사 학위논문

사람 단핵구에서 지질다당질에 의한 Kir2.2 이온통로의 조절 기전

Regulatory mechanisms of inwardly rectifying K^+ channel (Kir2.2) by lipopolysaccharide in human monocytes

2015 년 02 월

서울대학교 대학원

의과학과 의과학전공

김 경 수

A thesis of the Degree of Doctor of Philosophy

Regulatory mechanisms of inwardly rectifying K^+ channel (Kir2.2) by lipopolysaccharide in human monocytes

사람 단핵구에서 지질다당질에 의한 Kir2.2 이온통로의 조절 기전

February, 2015

The Department of Biomedical Sciences,

Seoul National University

College of Medicine

Kyung Soo Kim

사람 단핵구에서 지질다당질에 의한 Kir2.2 이온통로의 조절 기전

지도 교수 김 성 준

이 논문을 의학박사 학위논문으로 제출함

2014 년 10 월

서울대학교 대학원
의과학과 의과학전공
김 경 수

김경수의 의학박사 학위논문을 인준함
2014 년 12 월

위 원 장 _____ (인)
부위원장 _____ (인)
위 원 _____ (인)
위 원 _____ (인)
위 원 _____ (인)

Regulatory mechanisms of inwardly rectifying K^+ channel (Kir2.2) by lipopolysaccharide in human monocytes

by
Kyung Soo Kim

A thesis submitted to the Department of Biomedical Sciences in partial fulfillment of the requirements for the Degree of Doctor of Philosophy in Medical Science at Seoul National University College of Medicine

December 2014

Approved by Thesis Committee:

Professor _____ Chairman
Professor Kim, Sung Joon Vice Chairman
Professor Zhang Yin Hua
Professor Kang-Kyu Ye
Professor Kang, Tong Mook

ABSTRACT

Lipopolysaccharide (LPS) is effectively and widely used to stimulate Toll-like receptor 4 (TLR4) in monocyte. Ion channels are involved in the physiological and immunological responses of monocytes/macrophages. K^+ channels establish the negative polarized membrane potential and are critical for ion homeostasis in a variety of cells including monocytes. However, investigation on K^+ channels affected by LPS in monocyte is not completely understood. In THP-1 human monocytes treated with LPS (1 μg/ml), therefore, time-dependent changes of K^+ channels were investigated. Voltage-gated K^+ channel current (I_{Kv}) was decreased while Ca^{2+}-activated K^+ channel current (I_{KCa}) was increased after 6 h of LPS stimulation. Interestingly, inwardly rectifying K^+ channel current (I_{Kir}) was absent in the control cell, whereas it was appeared newly from 1 h, peaked at 4 h (−119 ± 8.6 pA/pF), and decayed to 27% of the peak at 24 h. Despite the presence of Kir2.1 and Kir2.2 mRNAs and proteins, the single channel conductance (38 pS) and Ba^{2+} sensitivity (IC_{50}, 1.42 μM) were consistent with Kir2.2. The functional upregulation of Kir2.2

was also confirmed in freshly isolated primary human monocytes. The results of immunoblot and confocal microscopy showed membrane translocation of Kir2.2 in LPS-treated monocytes whereas Kir2.1 expression is mostly retained in cytosolic. Moreover, $I_{Kir,LPS}$ was attenuated by the vesicular trafficking inhibitors. Both $I_{Kir,LPS}$ and plasma membrane translocation of Kir2.2 were inhibited by GF109203X (PKC inhibitor) or by transfection with siPKCε. Store-operated Ca^{2+} entry was augmented in the LPS treated THP-1, which was abolished by high K^+-induced depolarization. LPS-induced cytokine release (TNFα and IL-8) was weakened by ML-133, a selective Kir2 inhibitor. The spontaneously decayed $I_{Kir,LPS}$ at 24 h was reversed by PI3 kinase (PI3K) inhibitors (wortmannin and LY294002). In contrast, $I_{Kir,LPS}$ at 24 h was further suppressed by bpV(phen), an inhibitor for PTEN (PIP_3 phosphatase). However, $I_{Kir,LPS}$ at 24 h was not affected by Akt inhibitor, suggesting that the decay of $I_{Kir,LPS}$ was due to the decreased availability of PIP_2 itself, i.e. conversion into PIP_3 by PI3K. Dynamic reciprocal changes between PIP_2 and PIP_3 by inhibitors of PI3K and PTEN were confirmed using confocal microscopy for PLCδ-PH-GFP and Akt-PH-GFP expressed

THP-1 cells treated with 24 h of LPS. Taken together, to the best of our knowledge, these data are the first demonstration that Kir2.2 is functionally upregulated by TLR4 stimulation via PKCε-dependent membrane trafficking in human monocytes. And then, its current is spontaneously decayed by decreased availability of PIP_2 that is known to be critical for Kir2 activity. The augmentation of Ca^{2+} influx and cytokine release suggests a physiological role for Kir2.2 in the innate immunity of monocytes.

Keywords: monocyte, LPS, Kir2.2 channel, THP-1, PIP_2, PI3K

Student number: 2010-21899

CONTENTS

LIST OF TABLES AND FIGURES

Chapter 1

Chapter 2

Chapter 3

LIST OF ABBREVIATIONS

LPS : Lipopolysaccharide

TLR4 : Toll-like receptor 4

TNFα : Tumor necrosis factor alpha

IL-8 : Interleukin 8

Kv : Voltage-gated K^+ channels

KCa : Ca^{2+}-activated K^+ channels

Kir : Inwardly rectifying K^+ channels

I_{Kir} : Kir current

$I_{Kir,LPS}$: LPS-induced Kir current

PIP_2 : phosphatidylinositol-(4,5)-bisphosphate

PIP_3 : phosphatidylinositol-(3,4,5)-trisphosphate

PKC : Protein kinase C

PBMC : Peripheral blood mononuclear cells

PMA : Phorbol myristate acetate

PI3K : Phosphoinositide 3-kinase

PTEN : Phosphatase and tensin homolog

NF-κB : Nuclear factor kappa-light-chain-enhancer of activated B cells

MAPK : Mitogen-activated protein kinase

INTRODUCTION

Monocytes and macrophages are the major components of immunity and inflammatory response. Particularly, monocytes mediate host antimicrobial defense and are also implicated in wound healing, infection, and the pathophysiology of chronic inflammatory diseases such as atherosclerosis (Shi et al., 2011). In microbial infections, they are activated directly by pathogen-associated molecular patterns (PAMPs), for instance lipopolysaccharides (LPS), which are major components of the outer membrane of gram-negative bacteria (Dobrovolskaia et al., 2002). LPS activates CD14 · TLR4 · MD2 complex in monocytes/macrophages, resulting in the production of proinflammatory cytokines such as tumor necrosis factor (TNF)α, interleukin (IL)-1, IL-6, and IL-8 (Dobrovolskaia et al., 2002; Lu et al., 2008; Guha et al., 2001). Although cytokine production is important for the efficient control of invading pathogens, excessive activation of the innate immune system and the pro-inflammatory cascades may lead to septic shock and autoimmune disorders (Dobrovolskaia et al., 2002; Rittirsch et al., 2008; Troutman et al., 2012).

Functional expression and regulation of ion channels are involved in the physiological and immunological responses of monocytes/macrophages. For example, the transient receptor potential (TRP) family of non-selective cation channels and Orai family of Ca^{2+} channels are required for migration, differentiation and cytokine production of monocytes through changes in intracellular Ca^{2+} concentration ($[Ca^{2+}]_c$) (Colden-Stanfield et al., 2000; Schilling et al., 2009b; Wehrhahn et al., 2010; Floto et al., 1996). In addition to the Ca^{2+}-permeable channels, voltage-gated K^+ channels (Kv) and Ca^{2+}-activated K^+ channels (KCa) have been suggested to regulate proliferation (Qiu et al., 2002; Vicente et al., 2003; Eder, 2005), adherence (Erdogan et al., 2006; Colden-Stanfield, 2002), migration (Eder et al., 2005; Colden-Stanfield et al., 1998; Gendelman et al., 2009; Schilling et al., 2009a; Colden-Stanfield et al., 2000), differentiation (DeCoursey et al., 1996) and cytokine release (Qiu et al., 2002; Eder, 2005) in monocytes/macrophages. Generally, K^+ channels establish the negatively polarized membrane potential and are critical for ion homeostasis of cells, including immune system cells. In this study, Kir attracted our attention because Kir has been

reported in myeloid cells such as monocytes/macrophages rather those in lymphocytes. Owing to the high activity at the membrane voltage close to Nernst equilibrium potential of K^+ (K_{eq}), Kir are relatively effective player for setting the hyperpolarized membrane potential. Such hyperpolarization contributes to maintain and strengthen the Ca^{2+} influx (Colden-Stanfield et al., 1998; Franchini et al., 2004; Tare et al., 1998; Hibino et al., 2010).

THP-1 cells closely resemble human monocytes in their surface receptors and functional characteristics such as K^+ channels (DeCoursey et al., 1996; Qin, 2012; Kim et al., 1996). When treated with phorbol ester (a PKC activator), THP-1 cells differentiation into macrophage-like cells with a gradual emergence of Kir current (I_{Kir}) (DeCoursey et al., 1996; Kim et al., 1996). Expression of Kir has been commonly observed not only in macrophage but also in osteoclasts and microglia sharing the common myeloid origin (Eder, 2005; DeCoursey et al., 1996; Kim et al., 1996; Franchini et al., 2004). In macrophages, functional upregulation of I_{Kir} appears to be correlated with adherence (Colden-Stanfield et al., 1998; Colden-Stanfield et al., 2000), proliferation (Eder, 2005; Erdogan et al., 2006) and

cytokine production (Qiu et al., 2002).

As summarized above, a number of reports have described the expression and potential roles of K^+ channels in monocytes/macrophages. However, the effect of natural agonist for the Toll-like receptor 4 (TLR4), such as LPS on the K^+ channel activity in monocytes are unknown yet. Monocytes are also stimulated by pathological stimuli, releasing cytokines to recruit further immune responses (Shi et al., 2011; Dobrovolskaia et al., 2002). In a pilot experiment with THP-1 cells, we found that treatment with LPS induces Kir current ($I_{Kir,LPS}$) from null current within 1-4 hours while Kv amplitude is decreasing in the same time frame. Such a dramatic change of I_{Kir} is worth investigating to reveal the activation mechanism and molecular identity of $I_{Kir,LPS}$.

Among the seven groups of Kir family (Kir1 - Kir7), the Kir2.x subfamily shows strong inward rectification with background activity that is consistent with the recorded property of I_{Kir} in macrophages. Previous studies in human macrophages suggest that Kir2.1 is responsible for the recorded I_{Kir}. However, their conclusions are simply based on the Ba^{2+} sensitivity and strong rectification that are common

properties of other Kir2.x members (DeCoursey et al., 1996). Therefore, more precise investigation is still necessary to identify the molecular nature of I_{Kir} in monocytes/macrophages.

Although the activity of Kir2.x is not widely variable (i.e. providing a kind of background K^+ conductance near K^+ equilibrium potential), it can be also modulated by ions ($[K^+]_{ext}$), associated proteins and phosphatidylinositol-(4,5)-bisphosphate (PIP_2) in the plasma membrane (D'Avanzo et al., 2010; Fang et al., 2005; Hansen et al., 2011). In fact, Kir2.x are first investigated ion channels affected by electrostatic influence from negatively charged PIP_2 (Hibino et al., 2010). PIP_2 on the plasma membrane is distributed non-uniformly and may be located in raft-like domains and the substrate for phospholipase C (PLC) producing $InsP_3$ (Martin, 2001; Nam et al., 2007). Also, PIP_2 is converted to phosphatidylinositol-(3,4,5)-trisphosphate (PIP_3) by phosphoinositide 3-kinase (PI3K), which is a family of enzymes that regulate diverse immunological functions by stimulation such as LPS and TLR4 (Troutman et al., 2012; Guha et al., 2002; Okkenhaug et al., 2003). PIP_3 acts as a binding site for numerous intracellular enzymes that contain pleckstrin-homology domains (PH

domains) with selectivity for this lipid. Although PI3K is a key regulatory enzyme for a variety signals, the regulation of ion channels by PIP_2 conversion into PIP_3 is totally unknown.

In this study, we address the several following questions regarding human monocytes: (1) the molecular nature of Kir2.x, (2) the mechanism of the LPS-induced upregulation of I_{Kir}, and PI3K-dependent feedback regulation of I_{Kir} after LPS treatment. Our results demonstrate that TLR4 stimulation via LPS induces membrane trafficking of Kir2.2 in a PKCε-dependent manner, which causes dramatic increase of I_{Kir} in human monocytes. Furthermore, as a delayed response, we found that PI3K-dependent conversion of PIP_2 to PIP_3 reverses the initial upregulation of Kir2.2 activity. The upregulated I_{Kir} appears to positively regulate cytokine release as well as Ca^{2+} signaling in monocytes. This is the first report demonstrating the physiological role of Kir2.2 in primary cells and the regulation of ion channels regulated by conversion between PIP_2 and PIP_3. The modulation of Kir2 currents by LPS seems to be a potential target in the innate immune responses of monocytes.

MATERIALS AND METHODS

1. THP-1 cell culture and isolation of human blood monocytes

Undifferentiated THP-1 human monocytes were cultured in suspension with RPMI-1640 medium supplemented with 10% (v/v) fetal bovine serum and 1% penicillin/streptomycin at 37℃ in 5% CO_2 in a humidified incubator. Cells were sub-cultured 2-3 times per week. THP-1 cells within 25 passages were used in this study. Human peripheral blood mononuclear cells (PBMC) were isolated by density gradient centrifugation with Histopaque (GE Healthcare, Little Chalfont, United Kindom) from healthy volunteer after obtaining informed consent. Monocytes were then purified from PBMC by Spin-Sep™ human monocyte enrichment kits (Stem Cell Technologies, Canada) according to the manufacturer' s procedures. This work was approved by the Institutional Review Board of Seoul National University Hospital., according to the manufacturer's instructions. For patch clamp experiments, one-day incubated cells were cultured on either culture dish or coverslips.

2. Electrophysiology

Electrophysiological measurements were performed in the conventional whole-cell recording mode and cell-attached configuration at room temperature (22-25℃). Patch pipettes with a free-tip resistance of 3.5-5.0 MΩ were connected to the head stage of an Axopatch-200B patch clamp amplifier (Axon Instruments, USA). pCLAMP software v.9.0 and Digidata-1332A (Axon Instruments) were used to acquire data and apply command pulses. Suspension or coverslip-attached cells were transferred into a bath (approximately 0.15 ml) mounted on the stage of an inverted microscope (IX50; Olympus, Japan) and perfused with HEPES buffered Normal Tyrode (NT) solution at 5 ml/min. Single channel activities were recorded at 10 kHz in cell-attached configuration. Voltage and current data were low-pass filtered at 5 kHz. Current traces were stored and analyzed using Clamp v.10.2 and Origin v.7.0 software (OriginLab, USA).

3. Experimental solutions and chemicals

The pipette solution for whole-cell experiments contained 140

KCl, 10 HEPES, 5 NaCl, 5 EGTA, 0.5 $MgCl_2$ and 2 MgATP (in mM) and was of pH 7.2 adjusted with KOH. For some experiments, pipette solution contained free Ca^{2+} (300 nM) was used. The NT bath solution was composed of 145 NaCl, 10 HEPES, 5 glucose, 3.6 KCl, 1.3 $CaCl_2$, 1 $MgCl_2$ and 10 sucrose (in mM) and was of pH 7.4 adjusted with NaOH. To selectively evaluate the density of Kir current, 40K bath solution was used that contained 108.6 NaCl, 40 KCl (instead of 145 NaCl), and 3.6 KCl (in mM) in NT solution. The high K^+ bath solution for cell-attached mode contained the following (mM):140 KCl, 5 NaCl, 1 $MgCl_2$, 1.3 $CaCl_2$, 5 glucose and 10 HEPES (pH 7.4 with KOH); the pipette solution was composed 140 KCl, 5 NaCl and 10 HEPES (pH 7.4 with KOH). The internal pipette solution used for recording Ca^{2+}-release activated Ca^{2+} channel current (I_{CRAC}) contained (in mM) 125 Cs-glutamate, 20 CsCl, 10 BAPTA, 3 MgATP, 1 $MgCl_2$, 10 HEPES, 0.02 IP_3, and 0.002 sodium-pyruvate, and pH was adjusted to 7.2 with CsOH. The $CaCl_2$ concentration of bath solution was raised to 10 mM to measure I_{CRAC}. Stimulation of monocytes was performed in cell culture for 2, 4, 6 and 24 h at 37℃ in an atmosphere containing 5% CO_2 in cell culture medium in the presence of either 1 μg/ml

LPS (Sigma-Aldrich, USA) or 500 nM phorbol-12-myristate-13-acetate (PMA; Sigma). PI3K inhibitors, LY294002 and wortmannin (Sigma-Aldrich), PTEN inhibitor, bpV(phen) (Calbiochem), Akt signaling inhibitors, MK-2206 (Santa Cruz biotechnology) and SC-66 (Sigma-Aldrich), and tyrosine kinase inhibitor, genistein (Sigma-Aldrich) were included in the intracellular pipette solution during whole-cell patch clamp recordings. Other chemicals were from Sigma-Aldrich.

4. Membrane fractionation and western blot analysis

The protocol used for monocyte subfractionation was modified from that of Yin et al. (Yin et al., 2010). One-day incubated THP-1 cells were pretreated 1 μg/ml LPS for different durations. For membrane preparation, the LPS-treated cells were harvested and washed with phosphate-buffered saline (PBS). Cells were lysed in ice-cold lysis buffer at pH 7.5 containing 50 Tris-HCl, 5 EGTA, 2 EDTA, 5 DTT (in mM), 0.02% digitonin and a protease/phosphatase inhibitor cocktail (Roche Diagnostics, Mannhaim, Germany). The samples were

then frozen by floating the 1.5-ml tubes on a volume of liquid N_2 and thawed at room temperature. Cell lysates were then centrifuged at 14,000 ×g for 30 min at 4℃, and the supernatant, which comprised the cytosolic fraction, was removed. The pellet was then solubilized in an equal volume of the digitonin-based lysis buffer containing 1% Triton X-100 and centrifuged at 14,000 ×g for 30 min at 4℃, and the supernatant, which comprised the membrane fraction, was removed. An equal volume of Laemmli sample buffer was added to both fractions, and the fractionated proteins were resolved by 10% SDS-PAGE, followed by western immunoblotting.

To obtain total protein, cells were harvested and suspended in homogenization buffer containing 50 mM Tris-HCl (pH7.4), 100 mM NaCl, 5mM EDTA, 1% Triton X-100, and a protease/phosphatase inhibitor cocktail (Roche Diagnostics) for 1h at 4℃. The samples were centrifuged at 13,000 ×g, for 15 min at 4℃. Protein concentration was determined by the Bradford assay.

The protein samples were mixed with Laemmli sample buffer, resolved by 10% SDS-PAGE, and transferred to poly-vinylidene difluoride membranes in 25 mM Tris, 192 mM

glycine, 0.01% SDS, 20% methanol. Membranes were blocked in 1× TBS containing 1% Tween-20 and 5% bovine serum albumin (blocking solution) for 1 h at room temperature with gentle rocking, and incubated overnight at 4℃ with anti-Kir2.1, anti-Kir2.2 (Alomone labs, Jerusalem, Israel), and anti-Na^+-K^+ ATPase (Abcam, Cambridge, UK) primary antibodies followed by relevant secondary antibodies after washing. Blots were developed by ECL Plus Western blotting detection reagents (Amersham Bioscience, Piscataway, NJ, USA). Membranes were stripped using Pierce Restore Western Blot Stripping Buffer (Thermo Scientific, Waltham, MA, USA) for 30 min, and the relative densities were calculated after normalizing the intensity of each sample band to that of GAPDH.

5. RT-PCR

Prior to cDNA amplification, total RNA was isolated using TRizol (Invitrogen, Carlsbad, CA, USA) from THP-1 cells and human primary monocytes. Human Kir2.1-4 and β-actin mRNAs were analyzed using an established RT-PCR method. Briefly, 1 μg of total RNA was reverse-transcribed and the produced cDNA was amplified with 35 PCR cycles (55℃ for 0.5

min, 72℃ for 1 min, and 95℃ for 2.5 min). The nucleotide sequences of the primers used for amplification were summarized in Table 1. The PCR products were electrophoresed on a 2% agarose gel at 120 V in a 1× Tris-acetate-EDTA buffer and visualized using ethidium bromide.

6. Confocal immunofluorescence analysis

For immunofluorescence experiments, THP-1 cells were fixed with 4% paraformaldehyde in PBS for 30 min at room temperature. For Kir2 channel staining, cells were permeabilized with 0.1% Triton X-100 in PBS for 10 min, blocked in PBS with 10% fetal bovine serum for 1 h at room temperature, and incubated with anti-Kir2.1 or anti-Kir2.2 (respectively, 1:200) primary antibodies overnight at 4℃. The subcellular location of Kir2 channels was assessed using Alexa Fluor 488-conjugated (488 nm excitation, 1:500, Invitrogen) secondary antibody. Images were acquired using an Olympus FluoView FV1000 confocal microscope with a 100× oil-immersion objective.

7. Gene transfection and confocal imaging of PIP_2 and PIP_3

THP-1 cells transiently transfected with plasmids expressing enhanced green fluorescent protein (GFP)fused with the plexstrin-homology domain of either PLC δ (PH-PLC δ -GFP) or Akt (PH-Akt-GFP). The next day, the cells were treated with or without 1 μg/ml LPS for 24 h, and then plated onto poly-L-Lysine-coated glass bottom dishes. Laser scanning confocal microscopy with the Nikon NIS-elements A1 (Tokyo, Japan) and 60× oil-immersion objective was applied to visualize PH-GFPs (excitation 488 nm) in single cells treated with NT solution or 30 μM LY294002 for 30 min. The obtained images were analyzed using public domain software ImageJ (Wayne Rasband, National Institute of Health, Bethesda, MD, USA).

For suppressing PKC ε expression, si-PKCε RNA (siPKCε) was purchased from Cell Signaling Technology (Danvers, MA, USA). siRNA and GFP were transiently transfected using Nucleofector Kits and the corresponding protocols (AMAXA Biosystems, Germany), according to the manufacturer's

instructions for patch clamp recording and subfractionation.

8. Fura-2 fluorimetry and $[Ca^{2+}]_C$ measurement

$[Ca^{2+}]_C$ was measured using the fluorescent Ca^{2+} indicator Fura-2 acetoxymethyl ester (Fura-2 AM). THP-1 cells were loaded with Fura-2 AM (5 μM, 30 min, 25℃) and washed twice with HEPES-buffered physiological salt solution. Fluorescence was monitored in a quartz microcuvette (1 mL) with stirring in a in thermostated cell holder of a fluorescence spectrophotometer (Photon Technology International, Edison, NJ, USA) at excitation wavelengths of 340 nm and 380 nm, and an emission wavelength of 510 nm. At the end of each experiment, 5 μM ionomycin was applied to produce a maximum fluorescence ratio (R_{max}; 340/380 nm). Subsequently, 10 mM EGTA was added to confirm a minimum value of fluorescence ratio (R_{min}). The $[Ca^{2+}]_C$ values were calculated using the equation $[Ca^{2+}]c = K_d \times b \times (R - R_{min}) / (R_{max} - R)$, where K_d is the dissociation constant (224 nM) of Fura-2 AM and b is the ratio of the fluorescence excitation intensities of Fura-2 AM at 380 nm under Ca^{2+}-free and Ca^{2+}-saturated conditions.

9. Quantification of cytokines release

THP-1 cells pre-incubated in the absence or presence of Kir2 antagonist ML-133 for 30 min were stimulated with 1 μg/ml LPS for 4 and 8 h in humidified atmosphere (5% CO2, 37℃). Thereafter, culture supernatants were aspirated, centrifuged at 200 ×g for 10 min at 4℃, and stored at −80℃ until quantification of cytokines. Concentrations of IL-8 and TNFα were determined using the Bio-Plex 200 system (Bio-Rad, Hercules, CA, USA).

10. Statistical analysis

Data was managed and analyzed using Microcal Origin v.7.0 software (Marvern Instruments, Worcestershire, UK). Statistical results are presented as the mean ± standard error of the mean. Student's t-tests are used as appropriate to evaluate for significance, which was accepted for the p-value < 0.05.

RESULTS

Chapter 1

LPS-Induced Kir Current in THP-1 Monocytes

At first, the whole-cell currents were recorded in the unstimulated control THP-1 cells (control group). Ramp-like depolarization from -120 to 60 mV was applied to obtain current/voltage relationships (I/V curves) in an external solution consisting of either NT (HEPES-buffered normal Tyrode solution) or moderate high K (40 mM KCl; 40K). And then, the Ca^{2+}-activated K^+ (KCa) current was recorded by application of 50 μM 1-EBIO, a KCa3.1 activator, in NT condition. In the control group, both voltage-dependent K^+ (Kv) and KCa currents were dominant; inward current was negligible in either NT or 40K condition (Fig. 1A). To detect the acute effect of LPS on membrane conductance in THP-1, we compared I/V curves with 40K conditions before and 15 min after LPS (1 μg/ml) application. However no significant change was observed (Fig. 1B). Hereafter, the whole-cell currents and I/V curves were evaluated using the 40K condition.

The I/V curves of THP-1 cells exposed to LPS for different periods were compared; LPS-2h (1~3 h), LPS-4h (3~5 h),

LPS−6h (5~7 h) and LPS−24h (23~25 h), respectively (Fig. 1C). As described above, inward current was practically absent in the non−stimulated cells (−2 ± 0.4 pA/pF at −80 mV in 40K solution). Interestingly, a large I_{Kir} was observed in LPS−2h (−55 ± 8.1 pA/pF at −80 mV) that reversed at around −30 mV, close to the calculated Nernst equilibrium potential for K^+ at 40K. I_{Kir} was further increased in LPS−4h (−119 ± 8.6 pA/pF), and spontaneously decayed to −74 ± 13.5 and −32 ± 6.7 pA/pF in LPS−6h and LPS−24h, respectively (Fig. 1C and D).

On the other hand, well−observed Kv current in control THP−1 monocytes (17 ± 2.6 pA/pF) was attenuated by LPS, significantly decreased from LPS−6h; 8 ± 2.8 pA/pF and 5 ± 1.1 pA/pF in LPS−6h and LPS−24h, respectively (Fig. 2A, B). The I/V curves of 1−EBIO application showed both background K^+ and Kv conductance with a reversal potential close to −90 mV. Therefore, 1−EBIO sensitive current was displayed in Fig 2C and D by current subtraction of before and after 1−EBIO application. Interestingly, KCa conductance tended to increase according to LPS stimulation, and this change was significant from 6h of LPS incubation; 23 ± 4.8 pA/pF and 35 ± 5.4 pA/pF in LPS−6h and LPS−24h, respectively.

To elucidate dynamic regulation of I_{Kir} among changes of K^+ conductance by LPS, we investigated the tendency of Kir current regulation according to concentration and application time of LPS. Time-dependent $I_{Kir,LPS}$ was also observed at each condition of either application of one tens concentration of LPS (0.1 μg/ml) or wash-out condition after 0.5 or 1 hr of LPS stimulation (Fig. 3A and B).

Then we tested whether a stimulation of Toll-like receptor2 (TLR2) in monocytes (Dobrovolskaia et al., 2002; Guha et al., 2001) also affects I_{Kir}. THP-1 cells were stimulated with lipoteichoic acid (LTA), a TLR2 agonist, and I/V curves were analyzed for the same time period as above. Different from LPS, the LTA treatment did not induce I_{Kir} up to 24h (Fig. 4A and B).

Molecular Identification of LPS-Induced Kir Currents

To further characterize the molecular identity of $I_{Kir,LPS}$, unitary conductance and Ba^{2+}-sensitivity were analyzed by the whole-cell and cell-attached patch clamp recordings, respectively. In the LPS-treated THP-1 cells, cell-attached patch clamp recording with symmetrical [K^+] (140 mEq) consistently showed inwardly rectifying channel activities (Fig. 5A). No such channel activity was observed in the untreated control THP-1 cells. The unitary slope conductance of $I_{Kir,LPS}$

was 37.7 ± 1.42 pS (Fig. 5B) that is closer to the known conductance of Kir2.2 (35 to 40 pS) than the smaller ones such as Kir2.1 and Kir2.3 (Fang et al., 2011; Kubo et al., 2005).

Application of Ba^{2+} inhibited $I_{Kir,LPS}$ in a concentration-dependent manner (Fig. 5C and D, IC_{50}, 1.42 μM at −100 mV). According to recent studies, the IC_{50} of Ba^{2+} for Kir2.2 is lower than Kir2.1; IC_{50} for Kir2.1 ranges from 3−16 μM whereas Kir2.2 ranges from 0.5 to 2.3 μM (Fang et al., 2005; Hibino et al., 2010; Kubo et al., 2005). Therefore, we speculated that $I_{Kir,LPS}$ might be caused by Kir2.2 not Kir2.1.

The expressions of Kir2.1 and Kir2.2 transcripts and proteins were observed in THP-1 monocytes. RT-PCR analysis revealed mRNA expression for both Kir2.1 and Kir2.2 (Fig. 6A). Accordingly, the presence of Kir2.1 and Kir2.2 proteins was confirmed at each times of LPS incubation in THP-1 cells (Fig. 6B). Despite the robust I_{Kir} in LPS-treated cells, the amount of Kir2.2 protein from total cell preparation was not changed (Fig. 6B, lower panel).

LPS-Induces Kir2.2 in Primary Human Monocytes

THP-1 is one of the most widely exploited human cell line for the studies of monocytes (Schildberger et al., 2013; Qin, 2012) However, we determined whether the LPS-induced functional

upregulation of Kir2.2 is consistently found in human primary monocytes. In primary monocytes from human peripheral blood, there was no significant I_{Kir} before stimulation, while $I_{Kir,LPS}$ was consistently observed at around 2 h of LPS application, and decayed spontaneously at 24 h (Fig. 7A). The current densities at −80 mV were −13 ± 2.9 pA/pF, −54 ± 34.4 pA/pF, −196 ± 91.4 pA/pF and −41 ± 10.8 pA/pF at 2h, 4h, 6h and 24h, respectively (Fig. 7B). Albeit the timing of peak increase was a little delayed, the phasic changes of I_{Kir} were consistent with those of THP−1 cell. Cell−attached patch clamp also demonstrated Kir channel activity with 38.1 ± 1.39 pS of unitary conductance (Fig. 7C and D). In addition, we confirmed the expression of transcripts for Kir2.1 and Kir2.2, but not Kir2.3 and Kir2.4, in the primary monocyte (Fig. 7E). From the above results, we suggested that $I_{Kir,LPS}$ in both THP−1 monocytes and primary monocytes caused by Kir2.2 which would be related to role of physiological immune response.

Physiological Roles of I_{Kir} by LPS

The functional upregulation of I_{Kir} would hyperpolarize the membrane potential, providing the electrical driving force for Ca^{2+} influx through Ca^{2+}−permeable channels (Eder, 2005; Hinard et al., 2008). To confirm the hyperpolarization of

membrane potential by $I_{Kir,LPS}$, resting membrane potential (E_m) was measured in control and LPS-4h THP-1 cells. Non-stimulated cells showed no significant change of E_m (-31 ± 0.4 mV) before and after application of $BaCl_2$ (Fig. 8A and C), whereas E_m of LPS-treated THP-1 cells were hyperpolarized (-72 ± 1.7 mV) and depolarized by $BaCl_2$ (Fig. 8B and C).

To evaluate the plausible augmentation of Ca^{2+} influx by $I_{Kir,LPS}$-induced hyperpolarization, cytosolic Ca^{2+} concentration ($[Ca^{2+}]_C$) was measured in LPS-treated THP-1 cells. To fully activate store-operated (Ca^{2+} store depletion-activated) Ca^{2+} entry, thapsigargin (2 μM) was applied in the absence of extracellular Ca^{2+}. The inhibition of sarco/endoplasmic reticulum (ER) Ca^{2+}-ATPase by thapsigargin revealed a transient increase in $[Ca^{2+}]_C$ ($\Delta[Ca^{2+}]_{C,TG}$) reflecting the spontaneous release of Ca^{2+} from ER stores (Fig. 9A). The amplitude of $\Delta[Ca^{2+}]_{C,TG}$ was indistinguishable between control and LPS-4h groups (Fig. 9A). Subsequently, extracellular Ca^{2+} was replenished to 5 mM, which induced a sharp increase in $[Ca^{2+}]_C$ with slow decay to a plateau above initial level. The Ca^{2+} add-back after thapsigargin is a commonly used procedure to assess the store-operated Ca^{2+} entry (SOCE) in the immune cells (Floto et al., 1996). We also compared the

Ca^{2+}-release activated Ca^{2+} channel current (I_{CRAC}) in whole-cell patch clamp recordings. With $InsP_3$ (20 μM) and 10 mM BAPTA in the pipette solution, a spontaneous increase in inward Ca^{2+} current was observed in THP-1 cells. The reversal potential of I_{CRAC} was 40 mV, consistent with the Ca^{2+}-selective permeability. The I_{CRAC} density was unchanged in LPS-4h (Fig. 9B). Interestingly, despite the unaltered I_{CRAC}, both initial and steady-state SOCE were significantly higher in LPS-4h than in control (Fig. 9C and D). To evaluate the contribution of plausible membrane hyperpolarization by Kir upregulation, the above $[Ca^{2+}]_C$ measurement was repeated under 90 mM KCl (90K) conditions. The SOCE under 90K conditions was indistinguishable between control and LPS-treated THP-1, suggesting a role of enhanced electrical driving force for Ca^{2+} influx by Kir upregulation .

Increased Ca^{2+} influx modulated functional immune responses, such as cytokine production, inhibition of phagocytosis, expression of inducible nitric oxide synthase, stimulated respiratory burst and superoxide anion production in monocyte/macrophage (Colden-Stanfield et al., 2000; Schildberger et al., 2013). Most of all, LPS-stimulated monocytes produce cytokines such as TNFα, IL-1 and IL-8,

which, in turn, serve as endogenous mediators of inflammation through recruitment and receptor-mediated interactions with various target cells. Therefore, we examined if secretion of cytokines could be attenuated by inhibition of Kir2.2. Recently, a selective inhibitor for Kir2, ML-133, was reported (Wang et al., 2011). In LPS-4h cells, we confirmed that I_{Kir} was completely inhibited to 24% and 3% at -100 mV by 10 and 30 μM ML-133, respectively (Fig. 10A and B). Next, we compared the production of cytokines upon LPS stimulation between control and ML-133-treated THP-1 cells. TNFα and IL-8 were measured in the supernatant and normalized to the value at 4h (Fig. 10C and D). Basal secretion of TNFα and IL-8 was undetectable. Interestingly, both TNFα and IL-8 secretion by LPS was significantly decreased from 22 to 45% in the ML-133-treated cells. Thus, these results are reasonable to infer that Kir2.2 activation by stimulation of THP-1 with LPS is related to the immune response of monocyte activation through increasing Ca^{2+} influx and cytokine secretion via hyperpolarization.

Chapter 2

Membrane Translocation of Kir2.2 by LPS

Albeit the marked increase in I_{Kir}, the total protein level of Kir2.2 was unchanged (Fig. 1C and 6B). Therefore, we hypothesized that translocation of Kir2.2 to plasma membrane was responsible for the LPS-induced changes in I_{Kir}. Confocal Immunofluorescence microscopy showed that Kir2.2 was homogenously distributed throughout the cytoplasm in control cells. After LPS treatment, a distinctive staining pattern representing the translocation of Kir2.2 toward the cell periphery was observed and gradually increased according to over time of LPS stimulation (Fig. 11A). In contrast, Kir2.1-specific fluorescence signals were localized at intracellular clusters and were unchanged by LPS treatment up to LPS-24h (Fig. 11B). Also, the membrane trafficking of Kir2.2 was quantitatively analyzed using immunoblots after membrane fractionation (Fig. 12A). The Kir2.2 signal in the membrane fraction continuously increased up to 24 h while the constitutive membrane protein, alpha subunit of Na^+/K^+-ATPase, was unchanged (Fig. 12A). We also tested the effects of pharmacological inhibitors of vesicle translocation from endoplasmic reticulum (ER) to Golgi and plasma membrane

such as brefeldin A (BFA) and Exo-1 (Feng et al., 2003) on Kir2.2 translocation to plasma membrane. Both BFA and Exo-1 largely suppressed the I_{Kir} induction in LPS-4h (Fig. 12B).

PKCε-Dependent Trafficking of Kir2.2 in LPS-Stimulated THP-1 Cells

A previous report showed that PKC activation induces I_{Kir} in THP-1 cells (DeCoursey et al., 1996). Thus, we hypothesized that PKC might also be involved in $I_{Kir,LPS}$. To investigate whether the translocation of Kir2.2 by LPS was related with PKC activation, we measured $I_{Kir,LPS}$ incubating with pretreatment of PKC inhibitors. Three different types of PKC inhibitors (Gö6976, Gö6983 and GF109203X [GFX]) were applied 30 min before LPS treatment, and $I_{Kir,LPS}$ amplitudes at 4h were compared. Among them, GFX effectively suppressed $I_{Kir,LPS}$ by concentration-dependent manner; 1 μM: −60 ± 9.1 pA/pF and 10 μM: −24 ± 7.1 pA/pF at −80 mV, respectively (Fig. 13A and B). However, neither Gö6976 nor Gö6983 significantly attenuated $I_{Kir,LPS}$ (Fig. 13B). Also, we confirmed whether PKC-specific inhibition of Kir2.2 currents was reflected decrease of channel protein in the plasma membrane fraction. Consistent with the effects on electrophysiological change, the LPS-induced membrane translocation of Kir2.2

was also inhibited by GFX (Fig. 13C). According to the known relative potency of PKC inhibitors (Way et al., 2000), the above results suggest the involvement of PKCε isoform. PKCε is also known as a critical component of the TLR4 signaling pathway and thereby to play a key role in monocytes/macrophages and dendritic cells (DCs) activation in response to LPS (Aksoy et al., 2004; Comalada et al., 2003).

The correlation between PKCε activity and LPS-induced Kir2.2 trafficking to membrane was further proven by specific siPKCε transfection. Control or siPKCε was co-transfected with GFP vector in THP-1 cells. 48 or 72 hours after the transfection, the two groups of cells were further incubated with LPS-4h. We then performed whole-cell patch clamp in the GFP-positive cells under fluorescence microscopy. Consistently, in THP-1 cells transfected with siPKCε (72 h), the $I_{Kir,LPS}$ was significantly smaller to 45 % than in control scrambled siRNA-transfected cells (Fig 14A and B; from 116 ± 5.8 pA/pF to 64 ± 7.4 pA/pF). Furthermore, the membrane translocation of Kir2.2 was also inhibited by siPKCε transfection (Fig. 14C).

In order to measure translocation of Kir2.2, we take advantage of the fact that the cells surface area increases during the

fusion of the channel containing vesicle with the plasma membrane. In LPS-treated THP-1 cells, the electrical membrane capacitance, i.e. cell surface area, was increased almost by 50% (from 7.8 ± 0.23 pF to 11.5 ± 0.32 pF) at 4h of LPS-treated cells (Fig. 15A) which might reflect the active translocation of membrane vesicles to plasma membrane. Such increase in membrane capacitance was also suppressed by GFX, Exo-1 and BFA (Fig. 15B).

We also assessed whether PKC activation alone induced I_{Kir} in monocytes. Treatment with phorbol myristate acetate (PMA) actually induced significant I_{Kir} from 6 h up to 24 h without spontaneous decay of the current (Fig. 16A and B). The unitary slope conductance of Kir induced by PKC was 39.7 ± 4.10 pS (Fig. 16C and D). And the total protein level of PMA-induced Kir2.2 was qualitatively similar to that of LPS-induced which was not changed by PMA (Fig. 17A and B). These results indicated that LPS and PMA commonly induce Kir2.2 activity in human monocytes.

Chapter 3

PI3K Mediates the Spontaneous Decay of Kir2.2 Current in LPS-24h

The spontaneous decay of $I_{Kir,LPS}$ at 24 h of LPS treatment (LPS-24h, Fig. 1C and D) was inconsistent with the gradual increase in Kir2.2 protein in the membrane fraction (Fig. 10A). Thus, to investigate the spontaneous decay of I_{Kir} in LPS-24 h, we experimented according to two kinds of inferences: 1) endocytosis of Kir2.2, 2) decrease of Kir2.2 activity.

First, we measured $I_{Kir,LPS}$ with or without co-treatment of dynasore, an inhibitor of dynamin that is required for clathrin-mediated endocytosis (Young et al., 2009; Macia et al., 2006), after 4h of LPS stimulation (Fig. 18A). In fact, the $I_{Kir,LPS}$ at -80 mV was not affected by co-treatment with dynasore (Fig. 18B; 6h: -91 ± 14.4 and 24h: -25 ± 7.9 pA/pF, respectively)). In addition, the increase in membrane capacitance by LPS, an indicator of vesicle fusion to plasma membrane, was also persistently observed up to 24 h in the dynasore treated THP-1 cells (Fig. 18C). These results suggested that the decay of $I_{Kir,LPS}$ was not due to endocytosis.

It has been reported that Kir2.1 activity is modulated by phosphorylation at tyrosine residue (T242) in the C-terminal

domain that is commonly found in Kir2.x group (Hinard et al., 2008; Tong et al., 2001; Wischmeyer et al., 1998). However, the mean amplitudes of I_{Kir} in LPS−24h still showed spontaneous decay when co−treated with the tyrosine kinase inhibitor genistein (10 μM, 24 h)(Fig 19A). We also observed that an acute application of genistein (100 μM) in the pipette solution did not reverse the decay of I_{Kir} in LPS−24 (Fig. 19B).

It is also well−known that TLR4 signals lead to activation of PI3K and Akt−dependent signaling pathways, affecting various responses, including cell survival, proliferation and regulation of the pro−inflammatory in monocytes/macrophages (D'Avanzo et al., 2010; Guha et al., 2002). And, PI3K converts PIP_2 into PIP_3 by phosphorylation. Negatively charged phosphoinositol in PIP_2 binds to Kir2.x, which is critical for the activity (Hansen et al., 2011). The efficiency of PIP_2 in activating Kir2.2 is considerably higher than PIP_3 (Rohacs et al., 1999). Therefore, we hypothesized that the conversion of PIP_2 into PIP_3 by itself might explain the decreased I_{Kir} in LPS−24h. Bidirectional conversion between PIP_2 and PIP_3 is regulated by PI3K (PIP_2 → PIP_3) and PTEN (PIP_3 → PIP_2), respectively (Fig. 20A). To determine whether Kir2.2 activity could be also regulated by either decreased availability of PIP_2 or activation

of PI3K pathway, whole-cell patch clamp recording was carried out using inhibitors of PI3K (Okkenhaug et al., 2003; Ramos et al., 2005), PTEN (Schmid et al., 2004) and Akt (Hirai et al., 2010; Jo et al., 2011) including in the intracellular pipette solution. 24h of LPS-induced I_{Kir} from the first application of 40K after membrane break-in were compared with these from the 40K application after 10 min.

A treatment with Akt inhibitor, MK-2206, in the pipette solution did not change the amplitude of I_{Kir} in LPS-24h (Fig. 20B). Another Akt inhibitor, SC-66, also had no effect on I_{Kir} in LPS-24h (Fig. 20E). Interestingly, an acute treatment with PI3K inhibitor (30 μM LY294002) increased the amplitude of $I_{Kir,LPS}$, whereas the PTEN inhibitor, bpV(phen), further decreased the I_{Kir} in LPS-24h (Fig. 20C and D). When normalized to the initial amplitude of $I_{Kir,LPS}$ at -60 mV holding voltage in the whole-cell configuration, $I_{Kir,LPS}$ at 10 min after the treatment unequivocally showed the contrasting effects of bpV(phen) and PI3K inhibitors (LY294002 and wortmannin) (Fig. 20E). To confirm the time-course of PI3K activation by LPS treatment, the changes of amplitude of $I_{Kir,LPS}$ were measured at 2, 4, 6 and 24h by PI3K inhibitors in the pipette solution as described above. Normalized amplitude of $I_{Kir,LPS}$ at

was significantly unchanged at early phase of LPS treatment (2h and 4h) by both PI3K inhibitors (Fig. 21A and B). They only increased the amplitude of I_{Kir} in LPS-6h and LPS-24h cells.

Changes of PIP_2 and PIP_3 Levels on Plasma Membrane by LPS

To examine whether significant conversion of PIP_2 into PIP_3 by PI3K indeed occurs in LPS-24h, plecstrin homology (PH) domain containing fluorescence markers for PIP_2 (PH-PLCδ-GFP) and PIP_3 (PH-Akt-GFP) (Czech, 2000) were expressed in THP-1 cells. Each PH domain selectively binds to phosphoinositides of them and reflects PIP_2 and PIP_3, respectively. After treating with LPS for 24h, cells were analyzed by using confocal microscopy. At 30 min after applying LY294002, a significant increase in PH-PLCδ-GFP signal was observed in the peripheral region of LPS-24h (Fig. 22A) while no significant change was observed in the untreated control THP-1 cells (Fig. 22C). In contrast, PH-Akt-GFP signal showed a reciprocal decrease by LY294002 (Fig. 22B). No change of PH-Akt-GFP signal was also confirmed in control cells (Fig. 22D). To summarize the data, the fluorescence intensity of each PH-GFP in membrane region

was normalized to the initial level ($F_{Mem,30/Mem,0}$). In comparison to the relatively constant intensity of PH-PLCδ and PH-Akt in control cells (0.90 ± 0.04, 0.95 ± 0.039, respectively), PH-PLCδ-GFP and PH-Akt-GFP were significantly increased (1.21 ± 0.088) and decreased (0.71 ± 0.056), respectively, in LY294002-treated cells (Fig. 22E). Therefore, we suggested that the spontaneous decay of I_{Kir} after 24 h of LPS treatment was due to decreased availability of PIP_2 via conversion to PIP_3 by PI3K which is known to be critical for Kir2.2 activity.

Table 1. Nucleotide sequences of the primers used for RT-PCR

Protein (Gene)	Primer	Sequence (5' to 3')	Size (bp)
Kir2.1 (KCNJ2)	Forward	GGCTGTGTGTTTTGGTTGATAGC	648
	Reverse	ATAAGAGCTACGGCACTGTGTCG	
Kir2.2 (KCNJ12)	Forward	ACCCCTACAGCATCGTGTCA	237
	Reverse	AGATGAGCAGCATGTACCGC	
Kir2.3 (KCNJ4)	Forward	GACTTTGAGATCGTGGTCAT	237
	Reverse	CAGCACGGTGATCTTACTCT	
Kir2.4 (KCNJ14)	Forward	ACGTGCGTTTCGTAAACCTG	103
	Reverse	GAGAAGAGCAGGCACATCCA	

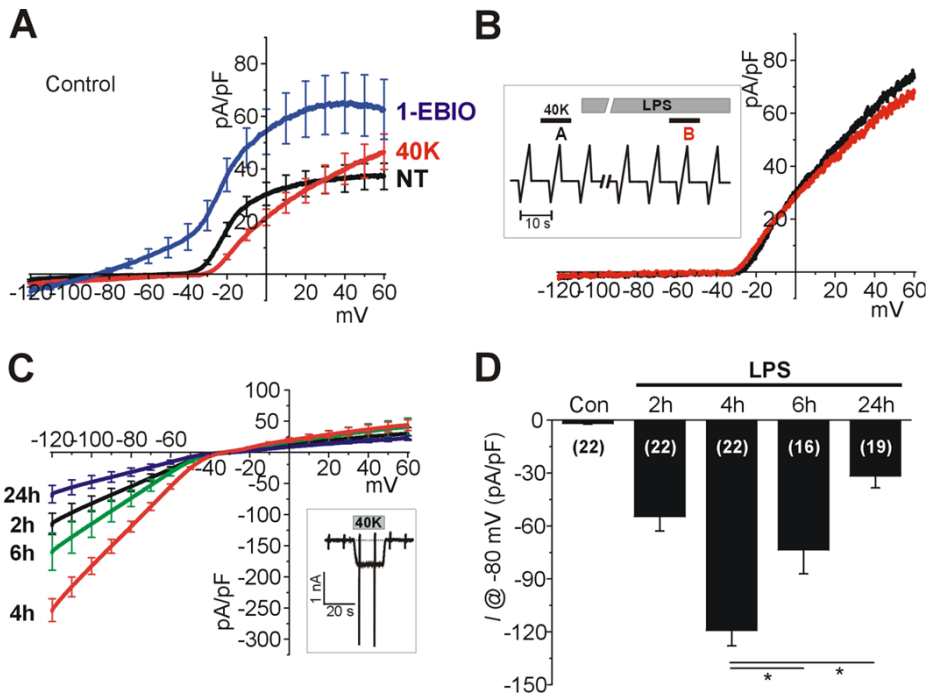

Figure 1. Induction of inwardly rectifying K^+ currents by LPS in THP-1 cells

(A) Averaged I/V curves of non-stimulated THP-1 cells in NT (black) and 40K (red; 40 mM of K^+) solution. Lastly, 50 μM 1-EBIO was applied at each recorded cells for KCa current recording (blue). (B) No significant change of I/V curves under 40K solution by acute application of LPS (1 μg/ml, 10 min). (C) Averaged I/V curves of LPS-treated THP-1 cells at 2, 4, 6 and 24 h in 40K solution (inset). (D) Summary of the I_{Kir} density at −80 mV. Number of recorded cells was indicated in each bar (means ± SEM, $*p<0.05$, unpaired Student's t test).

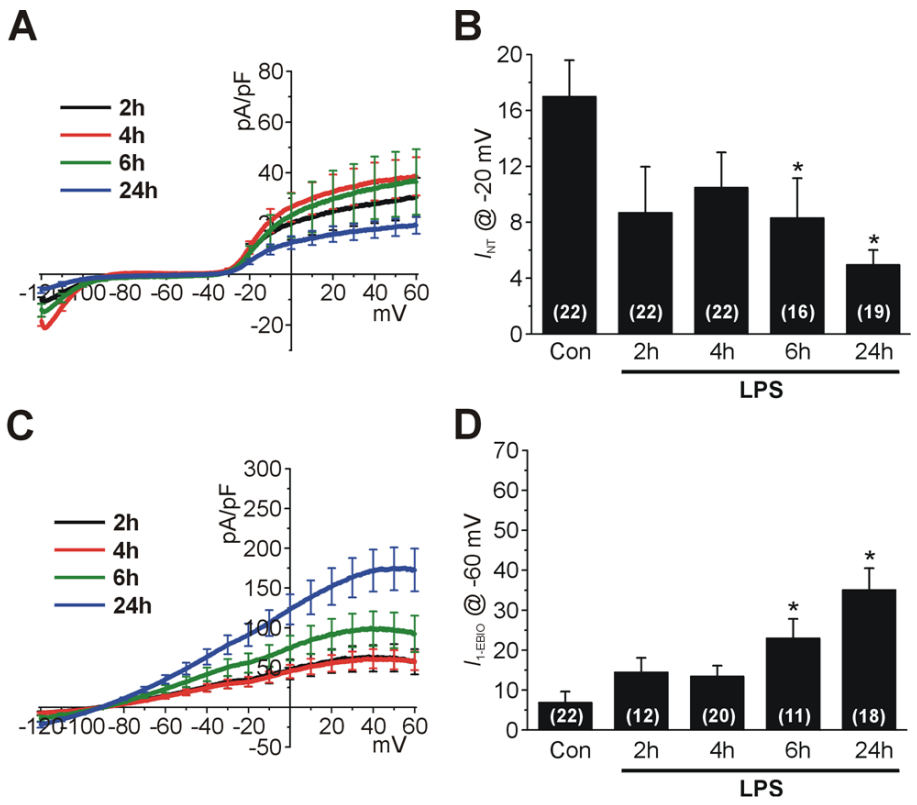

Figure 2. Time-dependent response of Kv and KCa currents by LPS stimulation in THP-1 cells

(A) Averaged I/V curves of Kv current density in LPS-treated THP-1 cells. (B) Summary of the Kv current density at -20 mV. (C) Averaged I/V curves of 1-EBIO sensitive current density (for KCa) in time-dependent incubation (2, 4, 6 and 24 h) with LPS were obtained using current subtraction of before and after 1-EBIO application. (D) Summary of the KCa amplitude at -60 mV was gradually increased by LPS application to 24 h. Number of recorded cells was indicated in each bar (means ± SEM, *p<0.05, unpaired Student's t test).

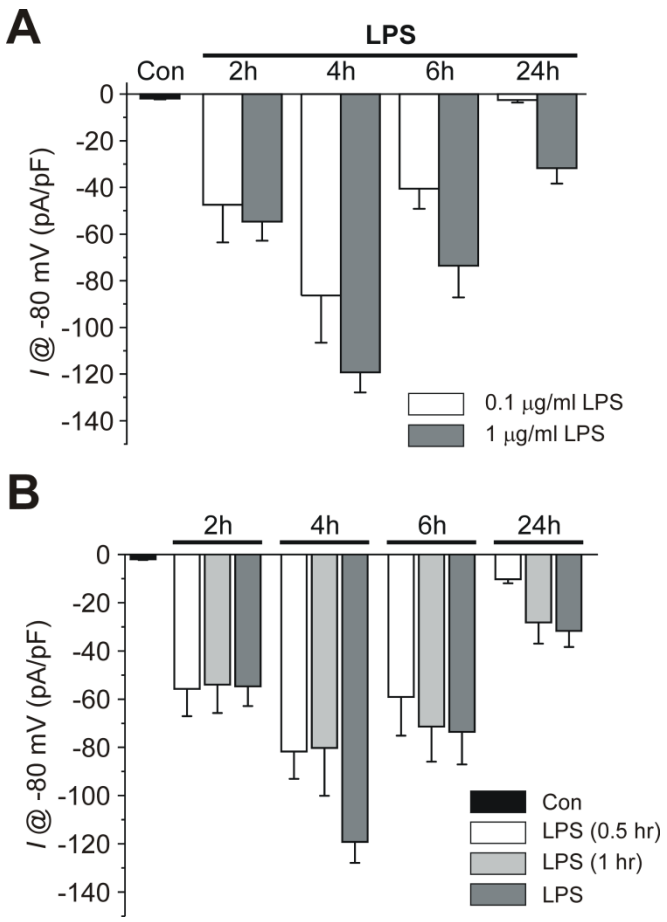

Figure 3. Response of I_{Kir} according to stimuli condition of LPS

(A) Summary of the time-dependent I_{Kir} density at −60 mV depending on LPS concentration. I_{Kir} of 0.1 μg/ml LPS stimulation at each time point (white bars) was slightly smaller than that of 1 μg/ml LPS, whereas their tendency of regulation was similar (n=3-9 in case of 0.1 μg/ml LPS, respectively). (B) Summary of the I_{Kir} density according to LPS application for 0.5 or 1 h (white bar and light grey bar, respectively). Biphasic regulation of I_{Kir} at each time point was observed regardless of LPS incubation time period. (n=5-8, means ± SEM).

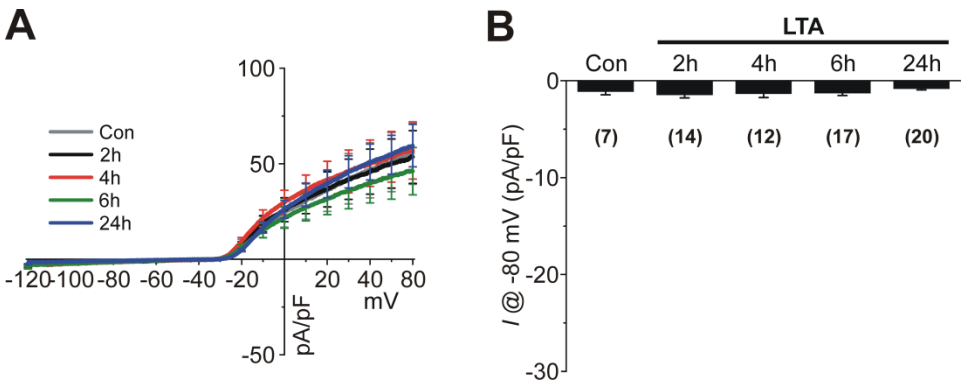

Figure 4. No effects of I_{Kir} by LTA stimulation in THP-1 cells

(A) Average I/V curves of control and LTA-treated THP-1 cells at 2, 4, 6 and 24h in 40K solution. Under whole cell-patch clamp, the membrane voltage was held at -60 mV and depolarizing ramp-like pulses (from -120 to 60 mV) were applied at every 10s. (B) Summary of the I_{Kir} density at -80 mV. Number of recorded cells is indicated in each bar. The current amplitudes are normalized to the membrane capacitance (pA/pF) and displayed with SEM (*p<0.05, unpaired Student's t test).

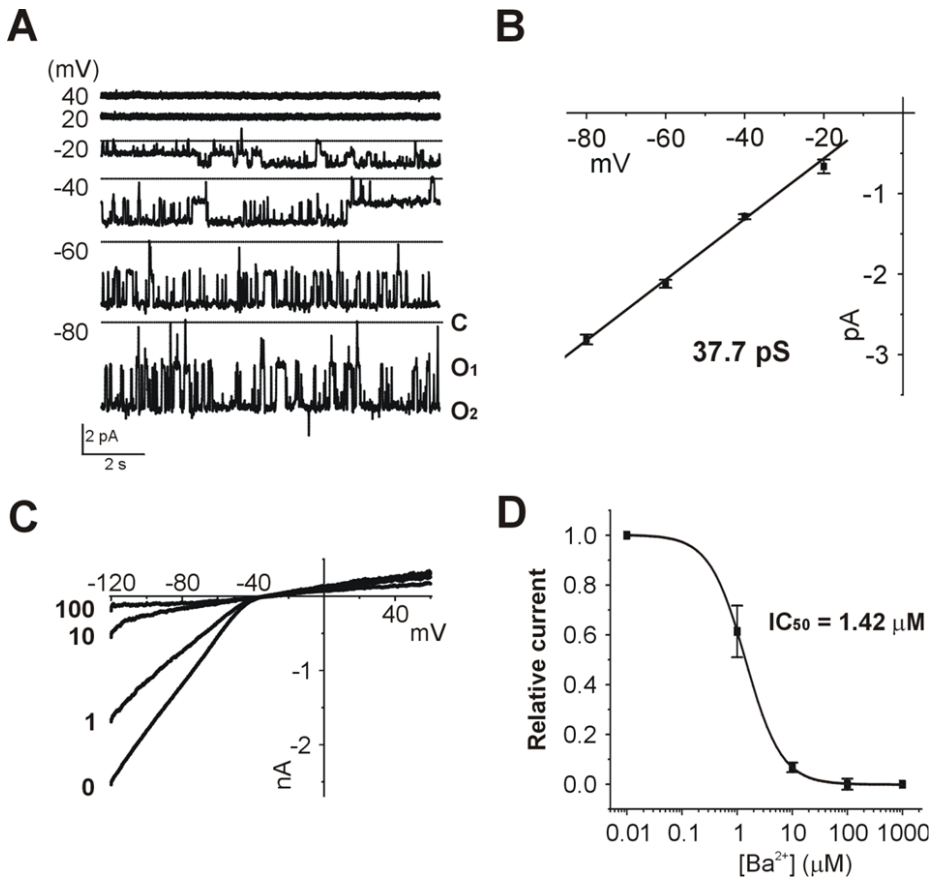

Figure 5. Electrophysiological property of $I_{Kir,LPS}$

(A) Representative current traces of cell-attached patch clamp recordings at different holding voltages in symmetric high K^+ condition. 'C', 'O_1' and 'O_2' indicate the closed and open levels of Kir channel, respectively. Two levels of current were observed at negative voltages (B) Averaged single channel amplitudes at negative voltages and their linear fitting yields 37.7 pS of slope conductance (n=4). Concentration-dependent inhibition of $I_{Kir,LPS}$ by Ba^{2+}. (C) Concentrations of Ba^{2+} (μM) are directly indicated in the representative I/V curves. (D)

Normalized amplitudes at −100 mV are summarized and fitted to a Logistic function. Dose dependent inhibition of Kir currents yielded an IC_{50} of 1.42 ± 0.405 μM (means ± SEM, n=4).

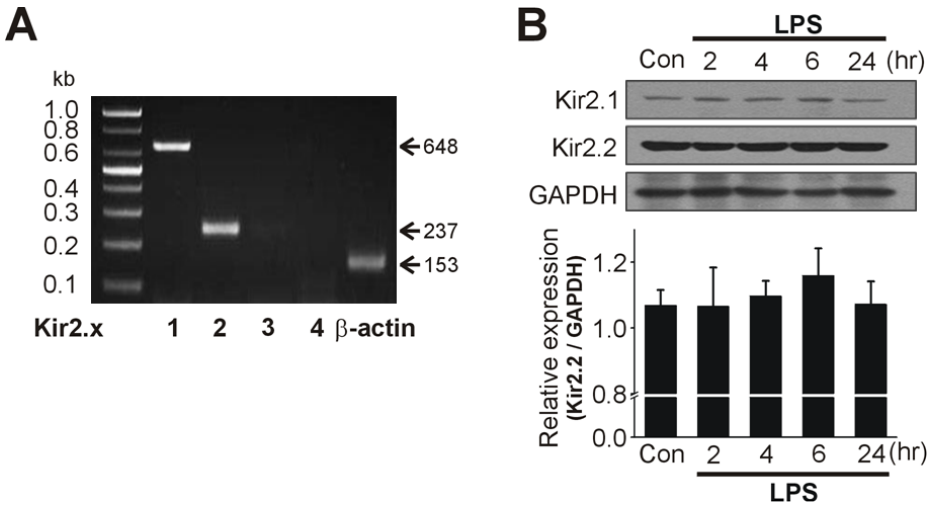

Figure 6. Molecular identification of $I_{Kir,LPS}$

(A) RT-PCR analysis for Kir2.1-4 in THP-1 cells. Positive signals corresponding to the expected sizes of Kir2.1 (648 b.p.) and Kir2.2 (237 b.p.) were detected while not for Kir2.3 and Kir2.4. β-actin (153 b.p.) was used as the control (rightmost lane). (B) Immunoblot assay for Kir2.1 and 2.2 in THP-1 cells. Cells were incubated in culture medium containing LPS for indicated periods, and then protein samples were obtained. Kir2.2 signal was normalized to that of GAPDH and the averaged values are displayed as bar graphs (n=6). Density ratios (Kir2.2/GAPDH) were indicated that the LPS-induced Kir2.2 activation was not caused by increase of their proteins (means ± SEM).

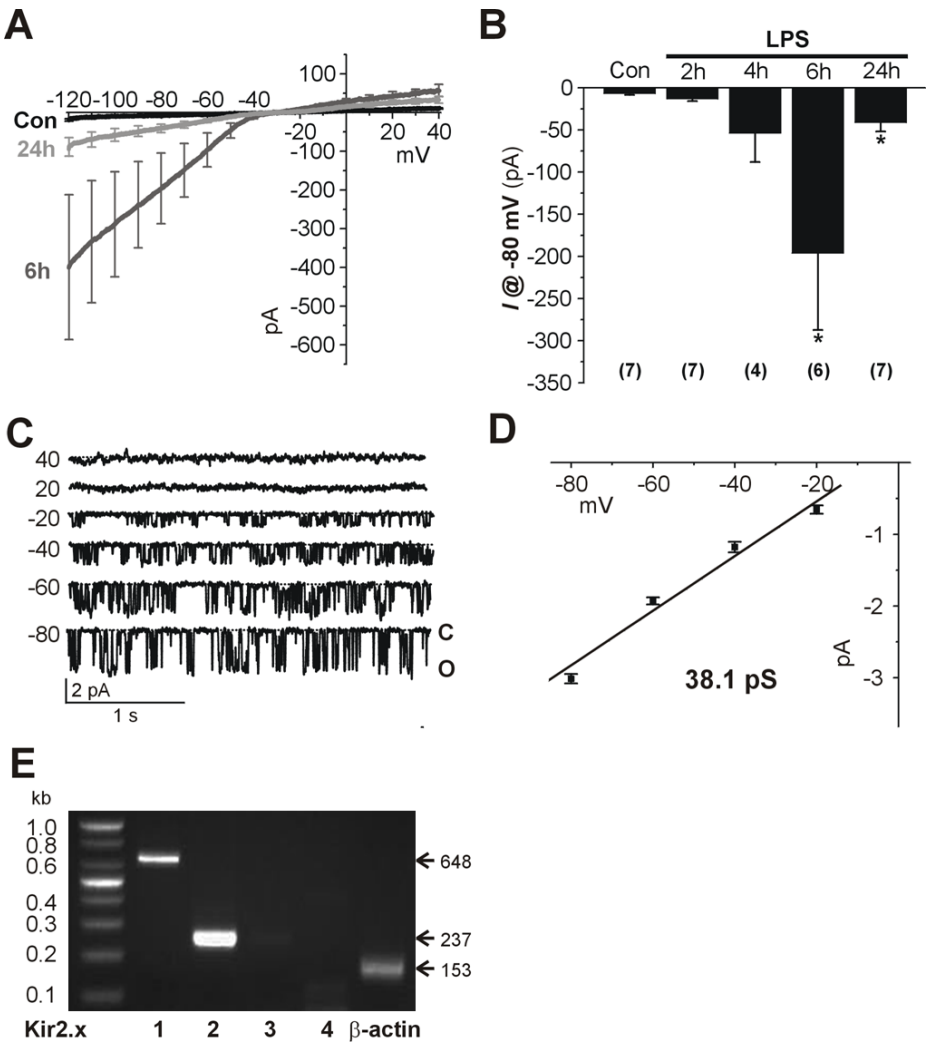

Figure 7. Increase of LPS-induced Kir currents in human primary monocytes

(A) The averaged I/V curves of whole-cell current in the control and LPS-treated human primary monocytes under 40K solution. (B) Summary of the I_{Kir} at −80 mV measured from primary monocytes incubated with LPS for different periods. Number of recorded cells was indicated below each bar (means ± SEM, $*p<0.05$, unpaired Student's t test). (C) Representative

traces of cell-attach single channel recording in primary monocytes under symmetrical K^+ conditions. Typical Kir currents recorded from primary human monocyte like THP-1 cells. **(D)** Averaged unitary current amplitudes at different voltages. The slope conductance was yielded 38.1 pS by a linear fitting. **(E)** RT-PCR detection of Kir2.1-2.4 in primary monocytes using same protocol with in THP-1 cells. Transcripts of Kir2.1 (648 b.p.) and Kir2.2 (237 b.p.) were positively detected their signals.

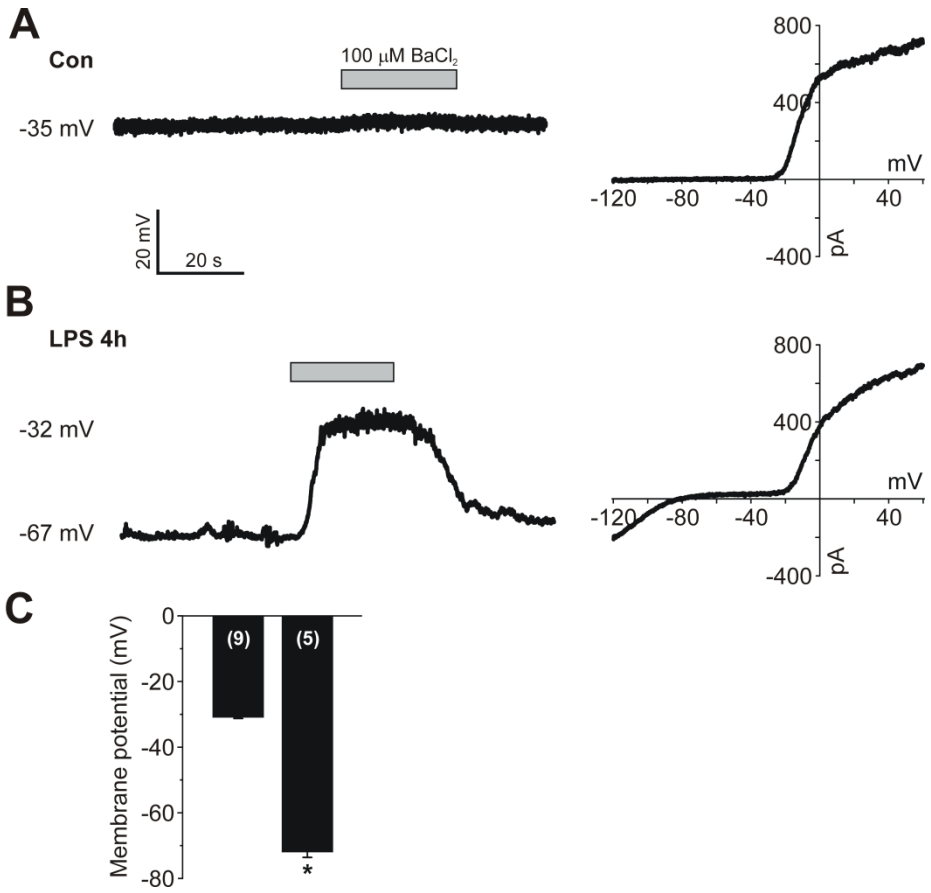

Figure 8. Effect of I_{Kir} on resting membrane potential of LPS-treated THP-1 cells.

(A, B) Representative of resting membrane potential recording in control (A) and LPS-treated THP-1 cells (B) before and after application of 100 μM $BaCl_2$. I/V curves were obtained by ramp-depolarization in each condition (right panel) before recording membrane potential. (C) Summary of resting membrane potentials recorded from different groups (means ± SEM, $*p<0.05$, unpaired Student's *t* test).

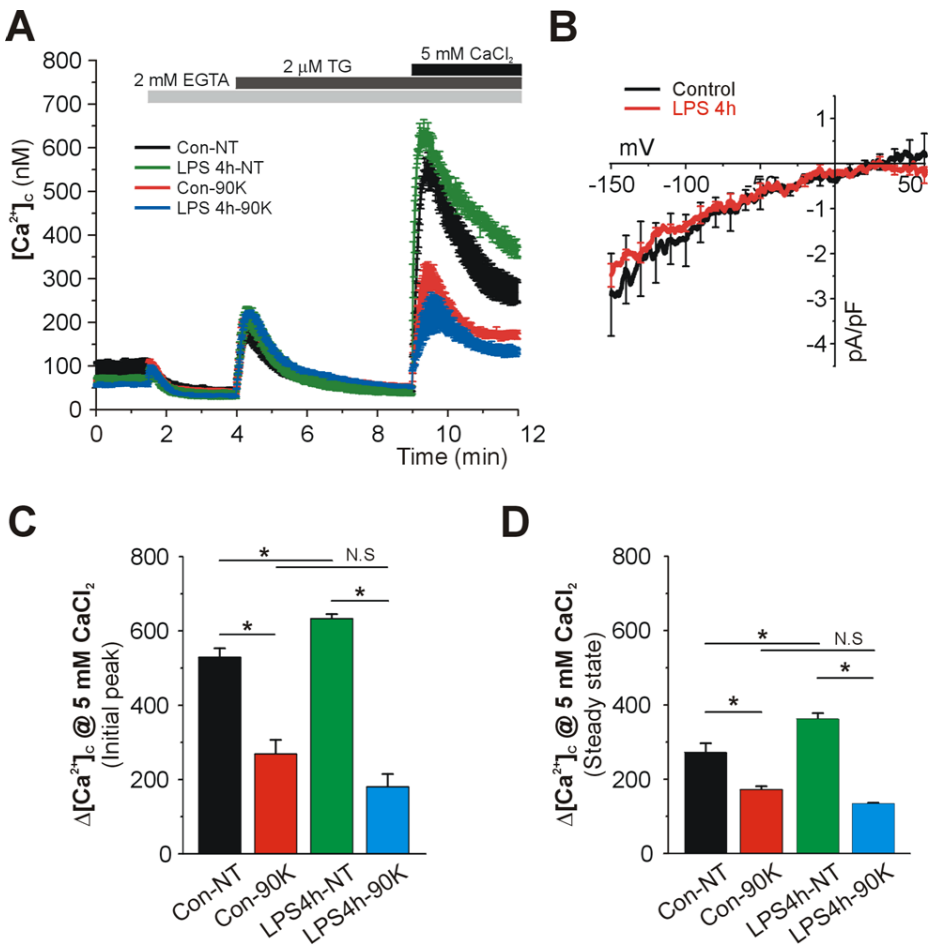

Figure 9. Effect of LPS-induced Kir currents on $[Ca^{2+}]_C$ in THP-1 cells

(A) Fura-2 loaded THP-1 cells were challenged with 5 mM $CaCl_2$ after chelating extracellular Ca^{2+} with 2 mM EGTA and ER depletion with 2 μM TG in either NT or 90K solutions (Ca^{2+} add-back procedure). The traces show the average responses calculated from two different conditions of cells (non-treated or 4h incubation of LPS). In each traces, Ca^{2+} add-back resulted in store-operated Ca^{2+} entry (SOCE) that was

composed of a peak followed by sustained $\Delta[Ca^{2+}]c$. **(B)** Comparison of CRAC currents (I_{CRAC}) between control and LPS-4h THP-1 cells. I/V curves of I_{CRAC} were obtained by ramp-depolarization at whole-cell configuration with 10 mM BAPTA and 20 μM $InsP_3$ in the pipette solution. The bath perfusate contains 10 mM $CaCl_2$ (n=3, respectively). **(C, D)** Summarized bar graphs of the initial peak (C) and sustained SOCE (D) were larger in LPS-4h cells in NT solution. In 90K solution, however, both peak and sustained SOCE were smaller and not increased in LPS-4h cells (n=5, $*p<0.05$, unpaired Student's *t* test).

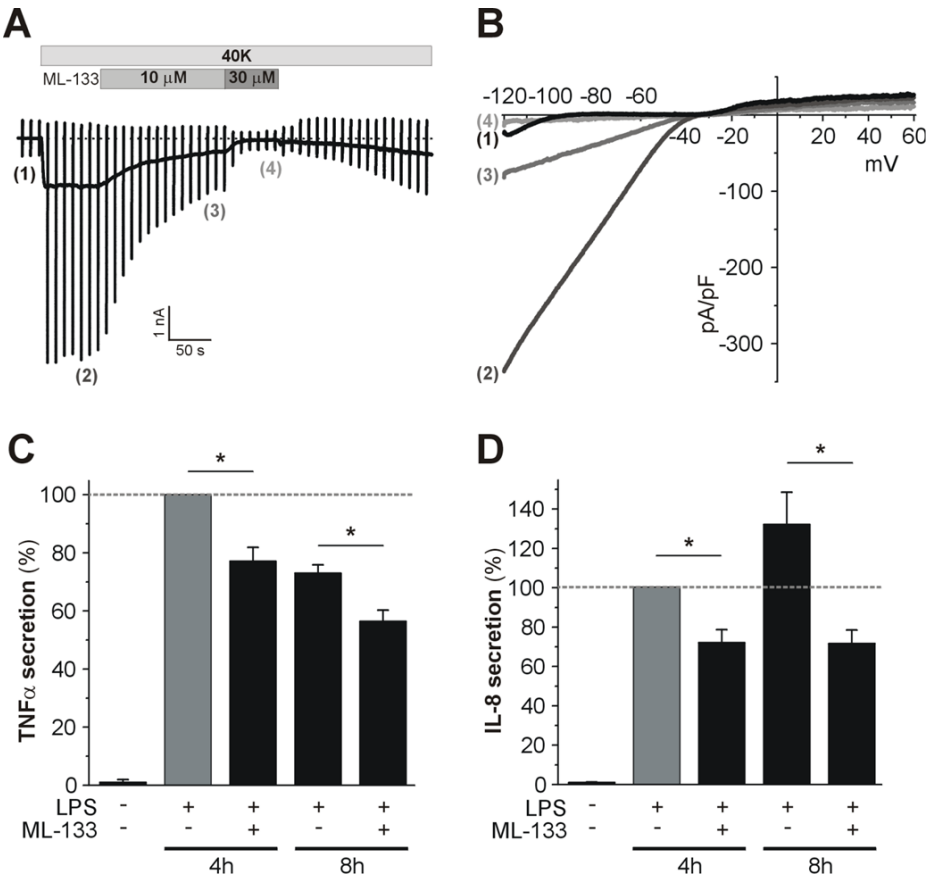

Figure 10. Attenuation of cytokine secretion by I_{Kir} inhibition in LPS-treated cells

(A) Inhibition of I_{Kir} by ML-133 in LPS-4h THP-1 cells. A representative time course of Kir2.2 currents measured at -60 mV holding voltage with repetitive ramp-like pulses from -120 to 60 mV. Applying 40K evoked the Kir currents within the range of command voltage and shifted the reversal potential, and then, 10 and 30 μM ML-133 was added, which resulted in complete inhibition of Kir2.2 currents. (B) I/V curves were

obtained in each condition. **(C, D)** Summary of cytokine release normalized to the amounts at LPS−4h only (gray bars) upon LPS−stimulated THP−1 in the present or absent of 30 μM ML−133. Both TNFα and IL−8 were almost absent in the control and released significantly at 4h and 8h of LPS treatment. 30 μM ML−133 commonly induced partial decrease of the cytokine release (n=5, $*p<0.05$, unpaired Student's *t* test).

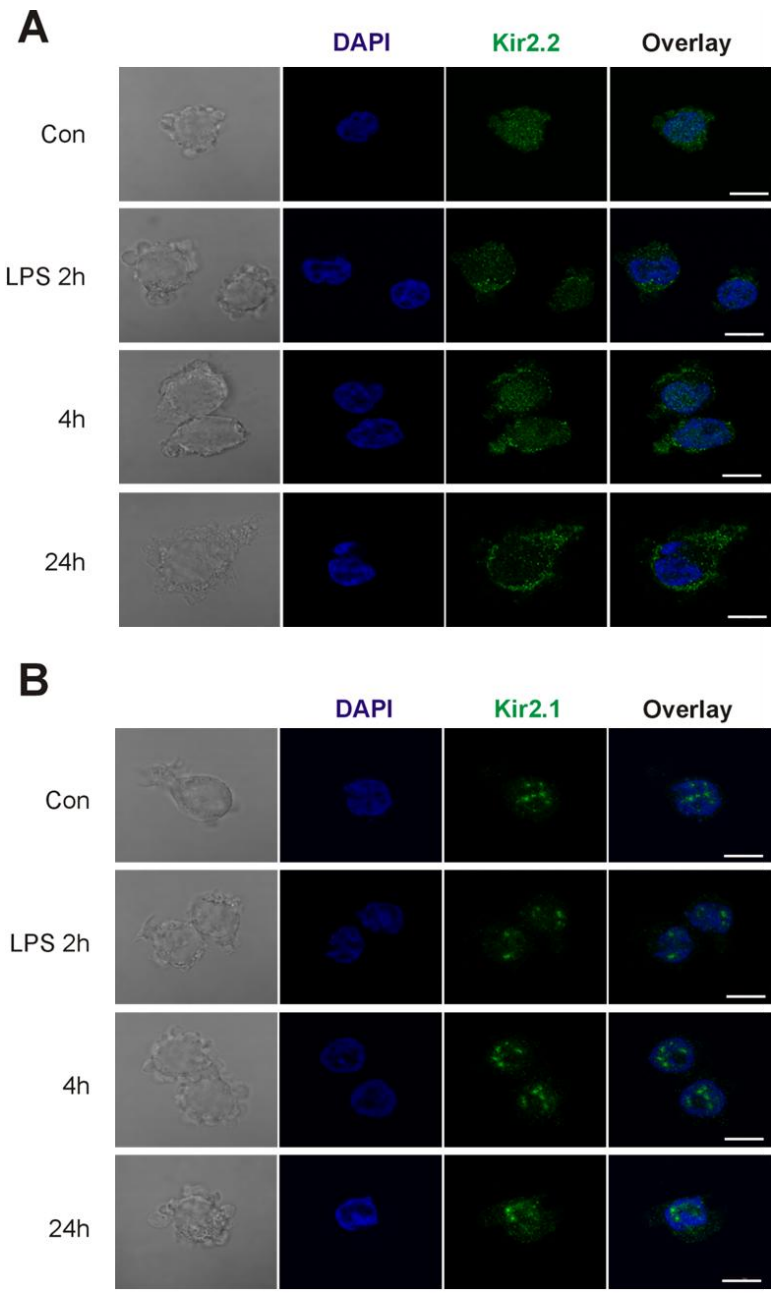

Figure 11. Confocal microscopy of Kir2.2 and 2.1 in LPS-treated THP-1 cells

(A, B) Representative immunofluorescence images using anti-Kir2.2 Ab (A) and anti-Kir2.1 Ab (B) in the THP-1 cell with or without 1 μg/ml LPS during indicating times (Con, 2h, 4h, and 24h, respectively). The translocation of Kir2.2 toward the cell membrane was observed over time, whereas Kir2.1 signals showed localization of intracellular compartments and unchanged by LPS treatment. The white bars of rightmost images indicate 10 μm of scale.

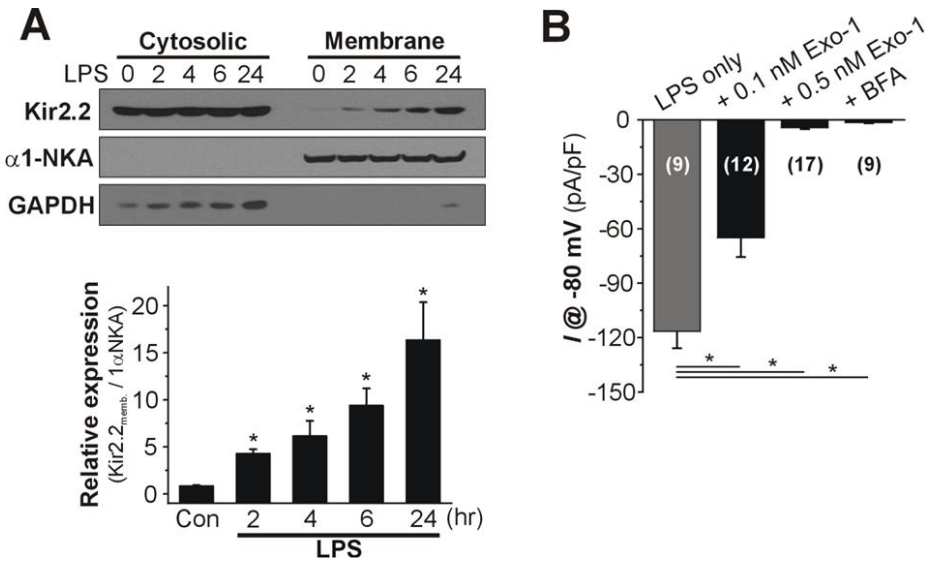

Figure 12. Upregualtion of I_{Kir} via membrane translocation of Kir2.2

(A) Representative immunoblots of Kir2.2 in the membrane and cytosol fractions (above), and quantitative analysis of Kir2.2 on membrane fraction from time-dependent LPS incubated cells (n=3, below). Membrane fraction Kir2.2 was increased by LPS over time. Na^+/K^+-ATPase-1 and GAPDH were used as a probes of membrane and cytosol fraction, respectively. (B) Summary of normalized $I_{Kir,LPS}$ density and inhibition by vesicle trafficking inhibitors, Exo-1 and BFA. Number of recorded cells was shown in the middle of bar graph. (means ± SEM, $*p<0.05$, unpaired Student's *t* test)

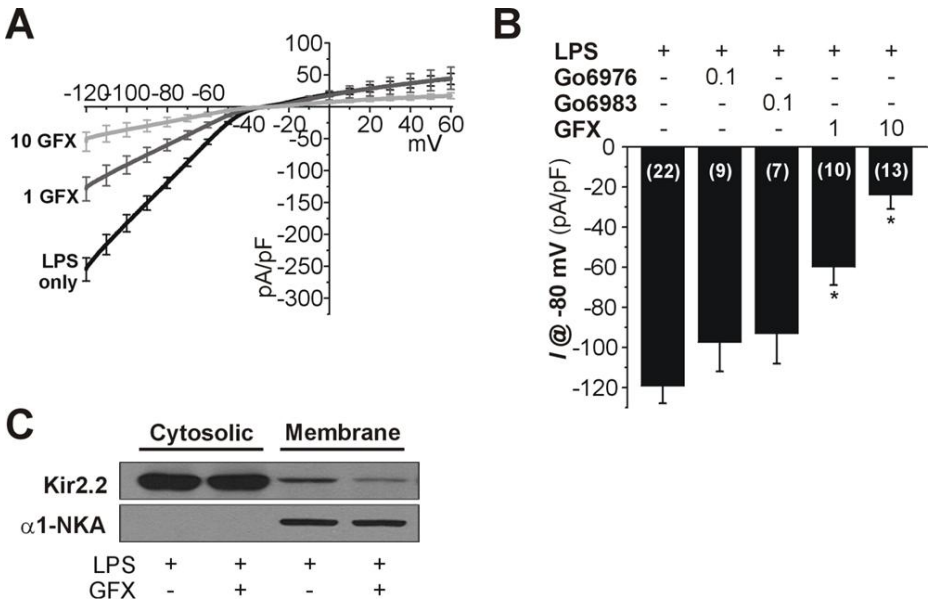

Figure 13. Translocation of Kir2.2 currents through PKCε-dependent membrane trafficking of Kir2.2

(A) Averaged I/V curves of $I_{Kir,LPS}$ recorded in control and GFX co-treated LPS-4h cells. (B) Summary of $I_{Kir,LPS}$ density (pA/pF at -80 mV) under control (LPS-4h) and co-treatment with PKC inhibitors (Go6976, Go6983 and GFX in μM). Only GFX among PKC inhibitors blocked the LPS-induced Kir currents. Number of recorded cells was indicated in each bar. (C) Representative immunoblot of cytosol and membrane fraction of Kir2.2. Trafficking of Kir2.2 to membrane by LPS was attenuated by application of 10 μM GFX. (means ± SEM, $*p<0.05$, unpaired Student's *t* test)

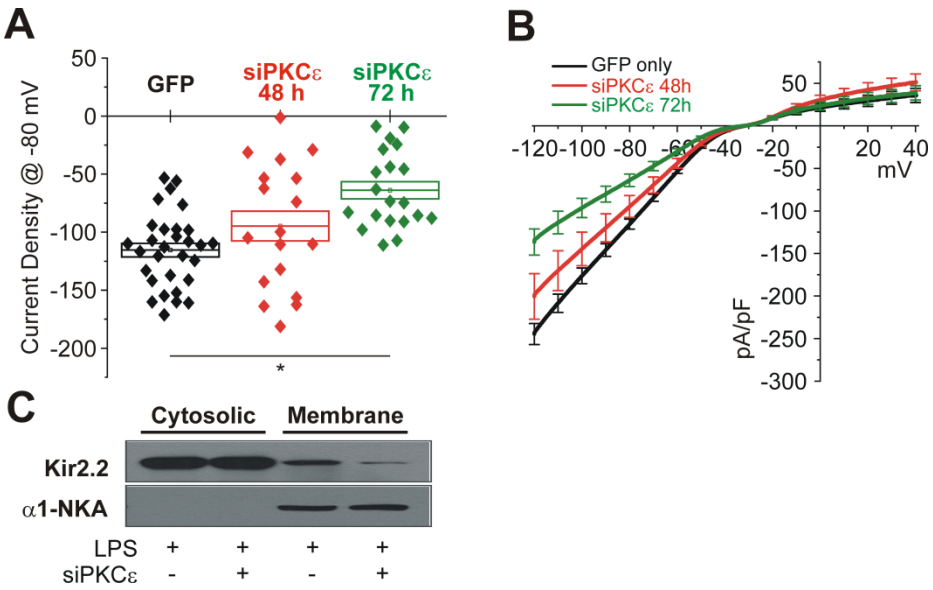

Figure 14. Effects of siPKCε on membrane trafficking of Kir2.2 in LPS-stimulated THP-1 cells

(A) Dotted $I_{Kir,LPS}$ density and means ± SEM (box) at −80 mV were indicated at each groups; GFP-only transfected cells (black, n=30), siPKCε transfection for 48 h (red, n=18) and 72 h (green, n=20), respectively. The currents of each group were obtained in LPS-4h THP-1 cells after transfection. In case of 72 h, current density was significantly inhibited by 45%. (B) Averaged I/V curves are shown that $I_{Kir,LPS}$ were inhibited in siPKCε transfected cells. (C) Representative immunoblot of cytosol and membrane fraction of Kir2.2. Trafficking of Kir2.2 to membrane by LPS was attenuated by transfection of siPKCε for 72 h. (means ± SEM, $*p<0.05$, unpaired Student's *t* test)

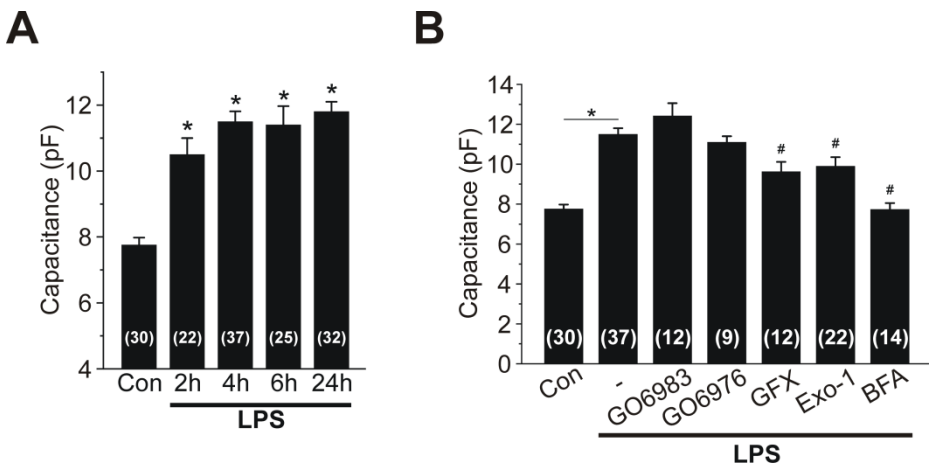

Figure 15. Changes of membrane capacitance by LPS and other inhibitors

(A) Summary of the averaged membrane capacitances (pF) at time-dependent LPS treatment. Membrane capacitances were immediately measured at whole-cell configuration before current recording and significantly increased by LPS application (from 2 h). (B) Summary of the membrane capacitances at each condition in LPS-24h THP-1 cells. In cases of GFX, Exo-1 and BFA among these inhibitors, increase of membrane capacitances were significantly inhibited. Number of recorded cells was indicated in each bar. (means ± SEM, all * and #p<0.05, unpaired Student's t test)

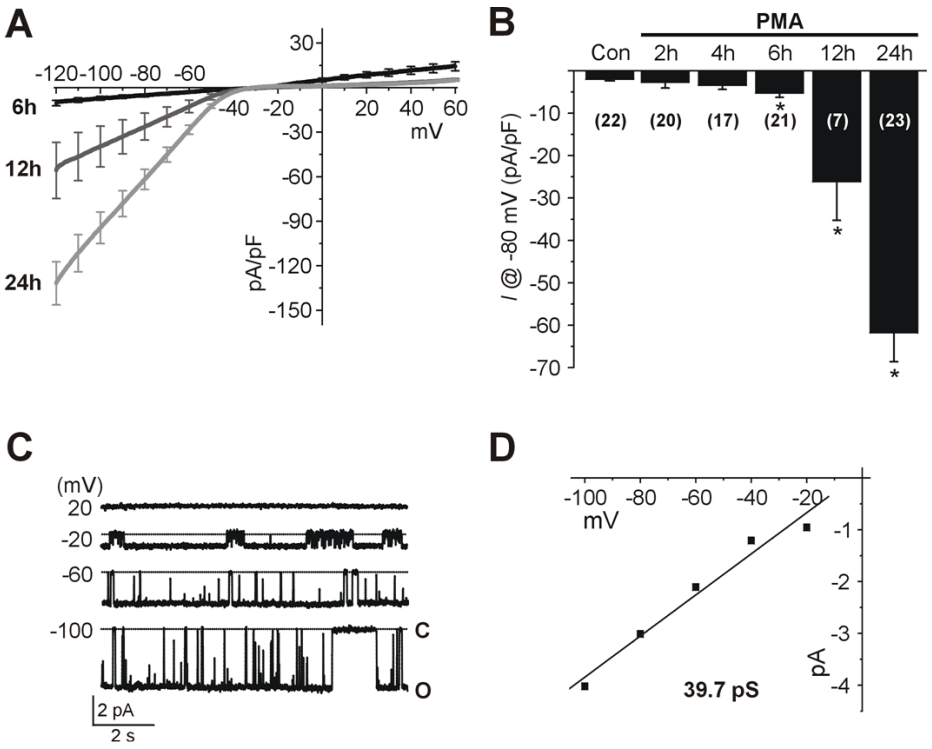

Figure 16. Induction of Kir2.2 activity by direct PKC activation

(A) Depolarizing ramp pulse (from −120 to 60 mV) was applied to obtain I/V curves at each time points (means ± SEM). The PMA−induced Kir currents ($I_{Kir,PMA}$) were continuously increased to 24 h of PMA incubation in THP−1 cells. (B) Summary of $I_{Kir,PMA}$ density (pA/pF, at −80 mV) exposed to 0.5 μM PMA for 2, 4, 6, 12 and 24 h. $I_{Kir,PMA}$ density were significantly increased from the first 6h, and consistently augmented to 24h. Number of recorded cells is shown in the middle of bar graph. (C) Representative single channel current

traces of 24h PMA-induced Kir currents in the cell-attach configuration of THP-1 monocyte. (D) The slope conductance of $I_{Kir,PMA}$ was measured by plotting of their currents at negative voltages and linear fitting (39.7 pS). (means ± SEM, $*p<0.05$, unpaired Student's *t* test)

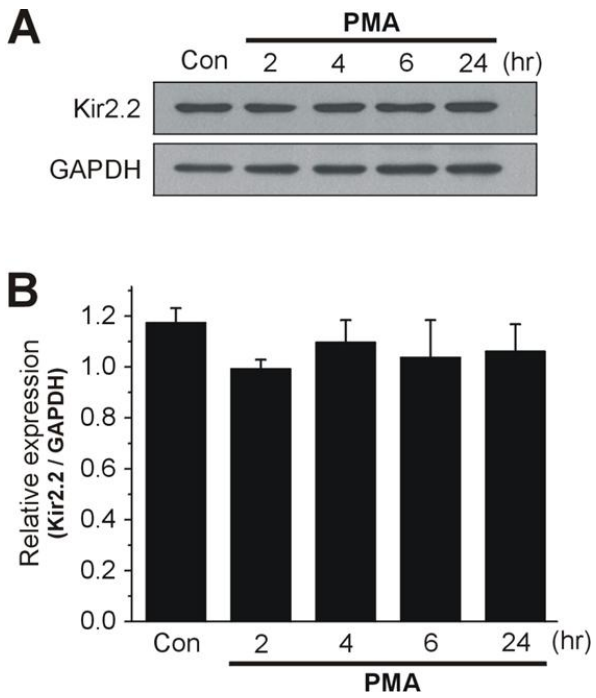

Figure 17. No change of Kir2.2 expression by PMA in THP-1 cells

(A) Immunoblot assay for Kir2.2 in PMA-treated THP-1 cells. Cells were incubated in culture medium containing 0.5 μM PMA for indicated times. (B) Summary of the immunoblot assay of Kir2.2. Density ratios (Kir2.2/GAPDH) were indicated that the $I_{Kir,PMA}$ was not caused by increase of their proteins (n=2, means ± SEM).

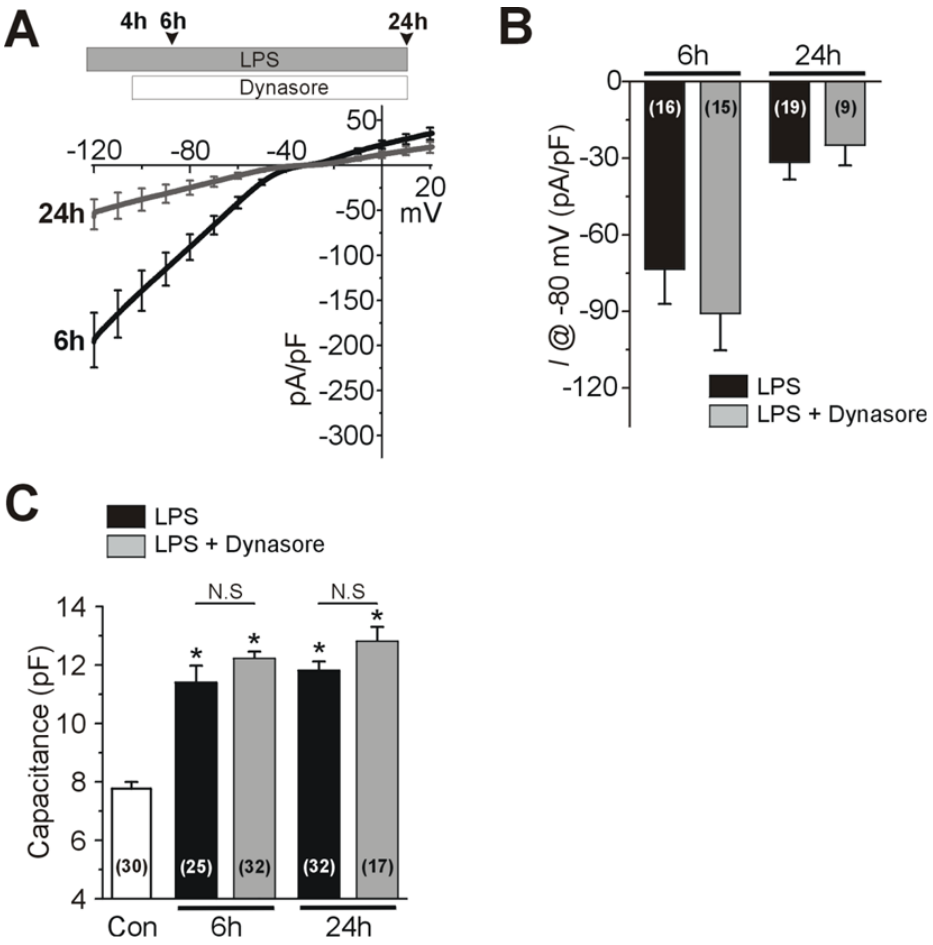

Figure 18. No effects of endocytosis inhibitor on the decay of $I_{Kir,LPS}$

(A) I/V curve of $I_{Kir,LPS}$ in LPS-6h and LPS-24h THP-1 cells with 30 μM dynasore, an inhibitor of endocytosis (see inset for the protocol). (B) Summary of $I_{Kir,LPS}$ density in LPS-6h and LPS-24h with or without dynasore co-treatment. Number of recorded cells is shown in each bar. (C) Summary of membrane capacitance (pF) of THP-1 cells in control, LPS-6h and LPS-

24h with or without dynasore co-treatment. Number of recorded cells was indicated in each bar. (means ± SEM, $*p<0.05$, unpaired Student's *t* test)

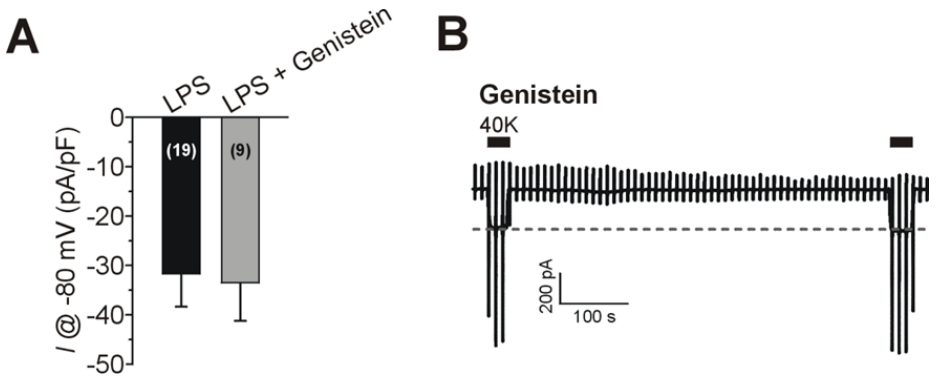

Figure 19. No effect of tyrosine kinase inhibitor on the decay of $I_{Kir,LPS}$

(A) Summary of $I_{Kir,LPS}$ density (pA/pF, at −80 mV). The amplitudes of Kir current in LPS−24h were not different between LPS−only (black bar) and genistein (grey bar) co−treated THP−1 cells. Number of recorded cells was indicated in each bar. (means ± SEM, $*p<0.05$, unpaired Student's *t* test) (B) Representative current traces with repetitive ramp pulses (−120 to 20 mV, every 10 s, −60 mV of holding voltage) in LPS−24 THP−1 cells. 40K bath solution was applied intermittently to evaluate the I_{Kir} amplitude changes during treatment with genistein (100 μM) in the pipette solution. at initial and after 10 min (black bar upper trace). Both current amplitudes of 40K application were not changed.

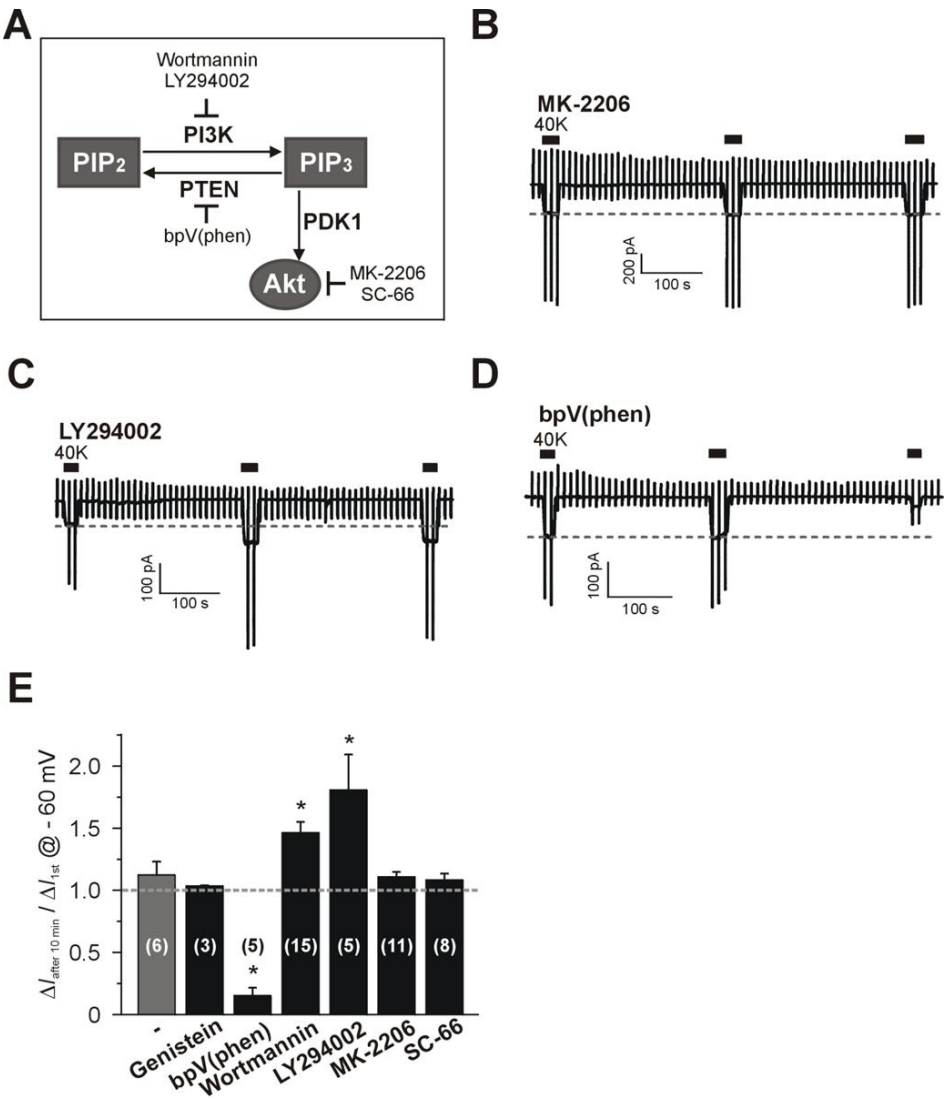

Figure 20. Spontaneous decay of $I_{Kir,LPS}$ via PIP_2 decrease by PI3K-dependent conversion into PIP_3

(A) Schematic diagram for the regulation of PIP_2 and PIP_3 conversion by PI3K and PTEN, and their inhibitors. PDK1 (3-phosphoinositide dependent protein kinase-1) is a kinase for the activation of Akt. (B, C, D) Representative current traces of

24 h LPS-induced I_{Kir} with repetitive ramp-like pulses (-120 to 60 mV, every 10 s, -60 mV of holding voltage) in whole-cell configuration applying 40K bath solution at initial and after 5 and 10 min (black bar upper trace)with the pharmacological agents. Each inhibitor was contained in the pipette solution (10 μM of MK-2206 (B), 30 μM of LY294002 (C) and 10 μM of bpV(phen) (D), respectively) to be dialyzed into cytosol. **(E)** Summary of $I_{Kir,LPS}$ change ratio induced by the drug application after the membrane break-in for whole-cell configuration. The inward current induced by 40K solution at 10 min was normalized to the one recorded 30 s after making whole-cell configuration. While genistein and MK-2206 had no effect, LY294002 and bpV(phen) induced significant decrease and increase of $I_{Kir,LPS}$ in LPS-24h cells. Wortmannin, another PI3K inhibitor, had positive effect similar to LY294002. Number of tested cells are shown in the middle of bar (means ± SEM, $*p<0.05$, unpaired Student's *t* test).

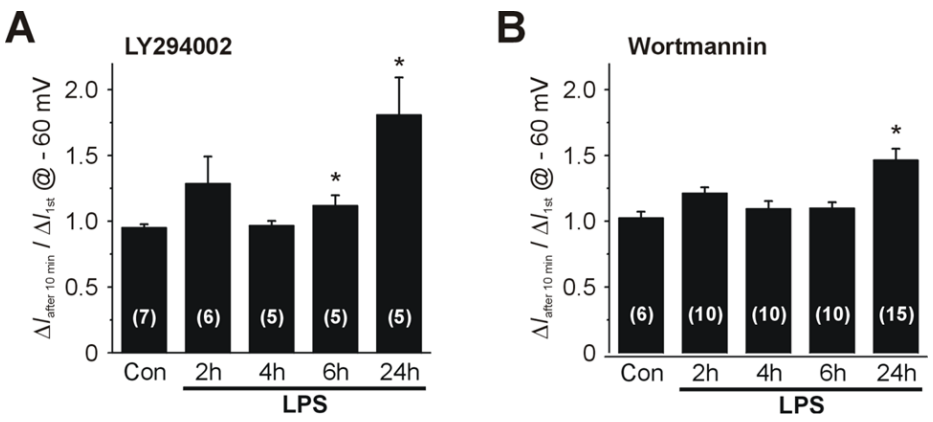

Figure 21. Changes of $I_{Kir,LPS}$ by PI3K inhibition

(A, B) Summary of the I_{Kir} change ratio induced by the PI3K inhibitors, LY294002 (A) and wortmannin (B), application after the membrane break-in for whole-cell configuration in control and LPS-treated THP-1 cells at 2, 4, 6 and 24h. Each inhibitor was contained in the pipette solution to be dialyzed in to cytosol. The inward current induced by 40K solution at 10 min was normalized to the one recorded 30s after making whole-cell configuration. Both PI3K inhibitors induced significant increase of I_{Kir} in LPS-6h and LPS-24h cells.

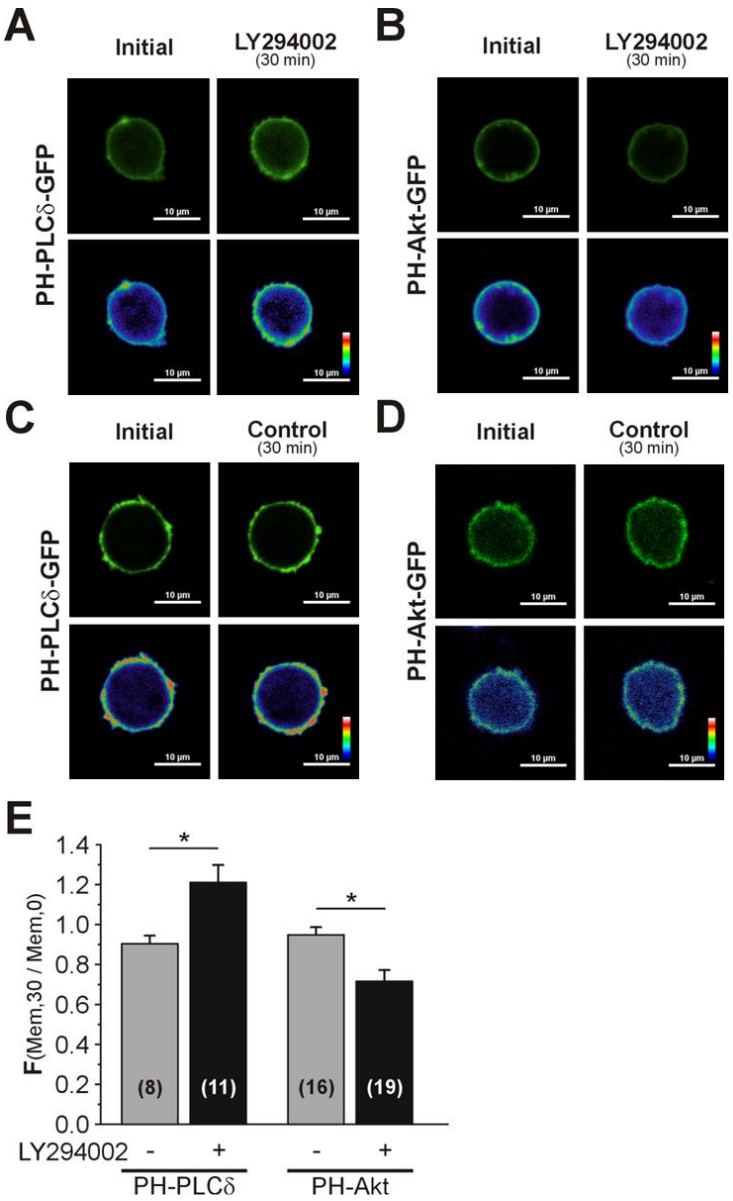

Figure 22. Confocal microscopy of PIP_2/PIP_3 levels in LPS-24h THP-1 cells and their changes by LY294002

(A, B) THP-1 cells were transfection with either PH-PLCδ-GFP for PIP_2 (A) or PH-Akt-GFP for PIP_3 (B), and then incubated with LPS for 24h. Confocal microscopy demonstrates

plasma membrane localization of PIP_2 and PIP_3 that are reciprocally increased and decreased by 30 μM LY294002 for 30 min, respectively. **(C, D)** Control cells recorded with 30 min interval without drug treatment show no significant change in the membrane signals for PIP_2 and PIP_3. Lower images of each panel displayed by the rainbow dark and white bars indicate 10 μm of scale. **(E)** Summary of fluorescence intensity of PH-PLCδ-GFP and PH-Akt-GFP measured along the membrane region of each cell. The fluorescence intensity at 30 min was normalized to the initial one (at 0 min) recorded in the same cell ($F_{(Mem,30/Mem,0)}$). The $F_{(Mem,30/Mem,0)}$ of PH-PLCδ and PH-Akt became increase and decreased by LY294002, respectively. Number of measured cells is indicated in each bar (means ± SEM, $*p<0.05$, paired Student's t test).

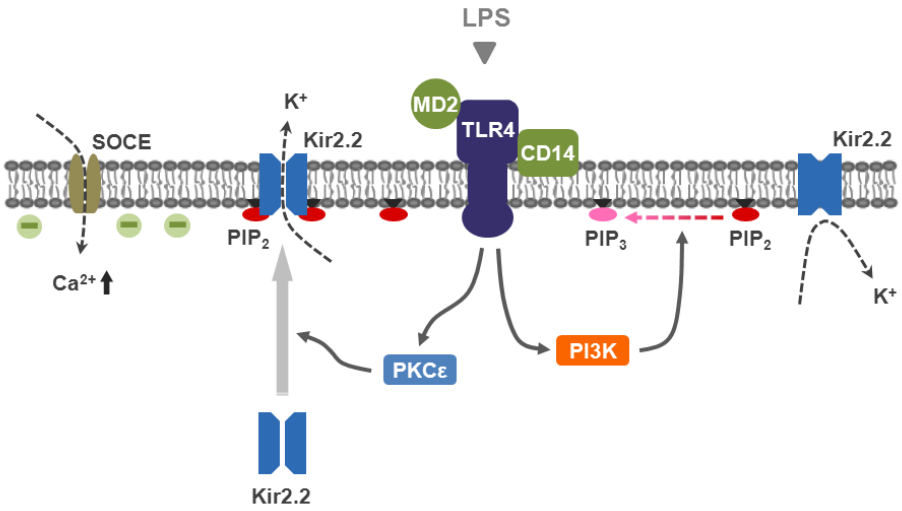

Figure 23. Schematic diagram of hypothesized mechanism for the modulation of I_{Kir} by LPS in human monocytes

The TLR4 stimulation via LPS induces membrane trafficking of Kir2.2 in PKCε-dependent signaling, which causes dramatic increase of I_{Kir} in human monocytes at initial phase within 4 h of LPS application. Nevertheless, the PI3K-dependent conversion of PIP_2 to PIP_3 reverses the initial upregulation of Kir2.2 activity. Finally, Kir current after 4 h of LPS stimulation was spontaneously decayed.

DISCUSSION

Our present study shows phasic changes in I_{Kir} in human monocytes stimulated by LPS and their underlying mechanisms, namely, initial activation by PKCε-dependent membrane trafficking of Kir2.2 and delayed inactivation by a PI3K-dependent PIP_2 decrease (Fig. 23).

The emergence of Kir2.2 activity provides hyperpolarized membrane potential, enhanced electrical driving force for Ca^{2+} influx, and facilitates the various immune responses such as cytokine production and Ca^{2+}-dependent monocyte functions. Although previous studies have demonstrated the functional upregulation of I_{Kir} in PMA- or M-CSF-stimulated macrophages and microglia (DeCoursey et al., 1996; Eder, 2005; Franchini et al., 2004), our study provides several novel findings: (1) the molecular identity of I_{Kir} as Kir2.2, (2) a PKCε-dependent translocation to plasma membrane, and (3) feedback inhibition of I_{Kir} by PI3K activation (Fig. 23). In the ion channel research field, the last finding is highly intriguing, because to our knowledge, this is the first example of regulation of channels by the putative conversion of PIP_2 and PIP_3.

Monocytes, related in innate immune response, are rapidly activated by stimulation within several hours. Not only the fully differentiated tissue macrophages but also circulating monocytes participate with a fast response to the microbial infection such as LPS. On this rationale, here we focused to the electrophysiological response of monocytes to LPS/TLR4 stimulation within 24h. I_{Kir} in THP-1 cells were rarely observed by acute application of LPS after whole-cell configuration, but its currents were induced from 2 h of LPS incubation, peaked at 4 h and spontaneously decayed 24 h (Fig. 1B and C). LPS-induced biphasic regulation of I_{Kir} was also preserved their patterns at both concentration- and time-dependent LPS application (Fig. 3A and B). A brief exposure to LPS (e.g. 0.5 or 1 hour of incubation and washout with fresh medium) was sufficient to induce I_{Kir} in THP-1 cells. These results suggested that the induction of I_{Kir} by LPS might be not a direct interaction with ion channel for activity but its regulation via complex LPS/TLR4 signaling cascades. LPS are widely used to stimulate TLR4, whereas other Toll-like receptors such as TLR2 might be also stimulated. In fact, TLR2 is known to be endogenously expressed in human monocytes

(Dovrovolskaia et al., 2002; Guha et al., 2001). However, I_{Kir} was not induced by the treatment with TLR2 agonist, LTA, which indicates that the induction of $I_{Kir,LPS}$ is TLR4-specific response (Fig. 4).

Identification of I_{Kir} in Human Monocytes

The four members of Kir2 (Kir2.1-2.4) show distinguishable unitary conductance; 20-30 pS for Kir2.1, 35-40 pS for Kir2.2, 10-15 pS for Kir2.3, and 14-15 pS for Kir2.4 (Fang et al., 2005; Kubo et al., 2005). While the presence of Kir2.1 and Kir2.2 mRNAs and proteins was confirmed in THP-1 and human monocytes (Fig. 6, 7 and 8), the unitary conductance of $I_{Kir,LPS}$ was close to that of Kir2.2 (Fig. 5B and 7D). Furthermore, the sensitivity of I_{Kir} to Ba^{2+} in the present study (1.42 μM of IC_{50}, Fig. 5D) was again closer to that previously reported property of Kir2.2 (IC_{50} of 0.5-2.3 μM) than Kir2.1 (IC_{50} of 3-16 μM) (Fang et al., 2005; Hibino et al., 2010).

To the best of our knowledge, this is the first finding of intrinsically expressed Kir2.2 in immune cells. In contrast to the numerous investigations regarding Kir2.1, the physiological role of Kir2.2 has been rarely investigated, except in the context of its co-expression with Kir2.1 in cardiomyocytes and

aortic endothelial cells (Fang et al., 2005; Kubo et al., 2005; Zaritsky et al., 2001). The unitary conductance of Kir2.1/Kir2.2 hetero-tetramer is known to be <30 pS (Hibino et al., 2010), which is different from the conductance of cloned Kir2.2 and the $I_{Kir,LPS}$. In addition, plasma membrane translocation of Kir2.1 was not observed in the LPS-treated THP-1 cells while Kir2.2 showed prominent time-dependent trafficking to plasma membrane (Fig. 10A). Taken together, it is highly likely that a homo-tetramer of Kir2.2, not a Kir2.1/2.2 hetero-tetramer, is functioning in human monocytes. To the best of our knowledge, this is the first functional finding of endogenous Kir2.2 in mammalian cells.

A previous report suggested that Kir2.1 is responsible for PKC-stimulated I_{Kir} upregulation in macrophages (DeCoursey et al., 1996). However, our study shows that the PKC activator PMA actually induces Kir2.2 channel activity (Fig. 16). In fact, the previous report (DeCoursey et al., 1996) did not confirm the specific isotopes using more precise phenotyping such as rigorous molecular analysis and unitary conductance analysis, as shown here. Despite the presence of Kir2.1 protein, the absence of single-channel activity corresponding to Kir2.1 is

confusing. Apparently, the plasma membrane expression or translocation of Kir2.1 is simply lacking in monocytes. It remains to be investigated whether there is another signaling pathway for recruiting Kir2.1 in monocytes/macrophages under different conditions.

Role of LPS-Induced I_{Kir} in Monocytes

In a variety of cell types, Kir have been identified and are presumed to have a role in the regulation of cell resting membrane potential (RMP) negative to the equilibrium potential for K^+ ions (Colden-Stanfield et al., 2000; Franchini et al., 2004; Tare at al., 1998). If the role of Kir2.2 on THP-1 cells is to maintain the membrane potential at a hyperpolarized level, its blocking should be set the RMP more positively, in turn, electrical driving force for Ca^{2+} influx was weakened. This was indeed the case, as clearly depicted in Fig. 8 and 9, since the Ca^{2+} influx via ER store depletion was faded off by 90K-induced depolarization. To support the Ca^{2+} influx, hyperpolarized membrane potential is required, and in this respect, the expression and upregulation of Kir2.2 would augment the Ca^{2+} signaling by LPS stimulation. Ca^{2+}-activated K^+ channels as well as Kir2.2 were also in charge of the

hyperpolarization of monocytes indicating a flux of K^+ ions out of the cells (Erdogan et al., 2006).

We could indeed show that inhibition of Kir2.2 resulted in an impaired secretion of TNFα and IL-8 (Fig. 10C and D). However, as Kir2.2 inhibition did not completely block cytokines secretion, the involvement of additional LPS signaling pathways might account for the residual cytokine release response such as TRPM2-mediated Ca^{2+} entry (Wehrhahn et al., 2010).

PKCε-Dependent Membrane Trafficking of Kir2.2

The present study provides multiple evidences that membrane translocation of Kir2.2 is responsible for the functional upregulation of $I_{Kir,LPS}$. Membrane proteins such as ion channels are synthesized in the ER, pass through a series of membrane-enclosed organelles including the Golgi complex, and are then trafficked via secretory granules to the plasma membrane (Bonifacino et al., 2004; Steele et al., 2007). Both confocal microscopy and immunoblot assay indicate that plasma membrane translocation of Kir2.2 is responsible for the $I_{Kir,LPS}$ (Fig. 11A and 12A). Consistently, pharmacological trafficking inhibitors such as Exo-1 and BFA effectively inhibited the

$I_{Kir,LPS}$ (Fig. 12B). Since the total amount of total Kir2.2 protein was not significantly changed by LPS, translational upregulation of Kir2.2 is not a likely mechanism for the response to LPS.

As for the intracellular signal triggering the putative trafficking of Kir2.2, the PKC pathway has attracted our attention, because treatment with the PKC activator PMA alone induced Kir2.2, albeit with a slower time course, in THP-1 cells (Fig. 16 and 17). Binding of LPS to the CD14/TLR4/MD2 complex activates a number of signaling cascades, predominantly leading to nuclear factor (NF)-κB, mitogen-activated protein kinase (MAPK), and multiple isoforms of PKC which causes secretion of proinflammatory cytokines (Aksoy et al., 2004; Comalada et al., 2003; Dobrovolskaia et al., 2002; Shapira et al., 1994). Besides, the essential roles of PKC have been established in many signaling systems of various cells, especially, involved in the regulation of protein trafficking to membrane (Akita, 2002; Muscella et al., 2008; Lan et al., 2001).

PKCs had known as a phospholipid-dependent serine/threonine kinase family, consisting of at least 11 isoforms that exhibit related homologies in their structures. The PKC isoforms can be classified into three main subfamilies

based on their second messenger requirements for activation: 1) conventional (cPKCs) α, βI, βII and γ; 2) novel (nPKCs) δ, ε, η and θ; and 3) atypical (aPKCs) ι/λ and ζ (Aksoy et al., 2004; Way et al., 2000). To examine whether PKC is involved in the membrane translocation of Kir2.2, three kinds of PKC inhibitors (Gö6976, Gö6983 and GFX) were tested. Gö6976 has selectivity for PKC and discriminates between cPKCs (α, β, γ) and nPKCs (δ, ε). Gö6983 preferentially inhibits cPKCs and PKCδ and PKCζ at nanomolar concentrations. GFX preferentially inhibits conventional PKCs (α, β) at concentrations below 1 μM, and also inhibits novel PKCs (δ, ε) at concentrations below 5 μM (Comalada et al., 2003; Muscella et al., 2008; Way et al., 2000). Among the three kinds of PKC inhibitors, only GFX effectively suppressed an induction of I_{Kir} and translocation of Kir2.2 to plasma membrane (Fig. 13). Based on the pharmacological selectivity of tested agents described above, it is most likely that PKCε is responsible for the Kir2.2 trafficking. This hypothesis was further examined by siPKCε transfection of THP−1 (Fig. 14). The essential roles of PKCε have been well established in many signaling systems including proliferation, differentiation, inflammatory, exocytosis

and translocation (Akita, 2002; Muscella et al., 2008). Besides, PKCε was found to be a critical component of TLR4 signaling pathway and thereby to play a key role in monocyte/macrophage and dendritic cells (DCs) activation in response to LPS (Aksoy et al., 2004; Comalada et al., 2003). Interestingly, the involvement of PKCs such as PKCε has been suggested in the membrane trafficking of an ion channel (NMDA receptor) and a transporter (pendrin) elsewhere (Lan et al., 2001; Muscella et al., 2008).

Although not rigorously investigated here, the increase in plasma membrane electrical capacitance in the LPS-treated monocytes membrane might also reflect the trafficking of Kir2.2-containing vesicles to the plasma membrane (Fig. 15 and 18C). In consideration of the fact that is the fusion of the vesicle containing ion channel with the plasma membrane, the cells surface area could increases, at least transiently.

PIP_2 Conversion by PI3K and Delayed Suppression of $I_{Kir,LPS}$

After the impressive increase at 4 h, the phenomenon of decaying $I_{Kir,LPS}$ raised a mechanistic question. Both the lack of recovery by the endocytosis-related GTPase inhibitor

(Dynamin), dyansore, treatment and the absence of a decrease in Kir2.2 protein amount in the membrane fraction suggest that a functional modification, rather than the protein expression in plasma membrane, was responsible for the spontaneous decay of $I_{Kir,LPS}$. However, tyrosine kinase inhibitor (genistein) could reverse the decayed $I_{Kir,LPS}$ at 24h (Fig. 19). The reason for using tyrosine kinase inhibitor is that Kir2.1 currents are inhibited by dephosphorylation of its tyrosine residue at position 242 (T242) of the Kir2.1 via tyrosine kinase phosphorylation, and recovered by tyrosine kinase inhibitor (Hinard et al., 2008; Tong et al., 2001; Wischmeyer et al., 1998). The T242 of the Kir2.1 is related to the channel activity and endocytosis (Jansen et al., 2008), and also present in Kir2.2 at equivalent positions. However, we could indeed show that $I_{Kir,LPS}$ at 24h was not inhibited by tyrosine kinase inhibitor, even if dephosphorylation of tyrosine residue is occurred.

Such inconsistence required functional modification of Kir2.2 activity is additionally induced by prolonged LPS/TLR4 signaling. After excluding the endocytosis- or kinase-dependent modulation mechanisms, we hypothesized that the PIP_2, critical regulator of Kir2.2 activity, might be changed by

PI3K, which is well known to be activated by LPS/TLR4 signaling (Okkenhaug et al., 2003; Ramos et al., 2005; Troutman et al., 2012). For these processing, PIP_2 should be converted to PIP_3 as signaling mediators via PI3K activation. Inhibition of the PI3K/Akt pathway in human monocyte enhances MAPK and its downstream targets of LPS signaling, but activation of that pathway limits TNFα expression (Guha et al., 2002). Therefore, the reciprocal changes in $I_{Kir,LPS}$ by PI3K inhibitors (LY294002 and wortmannin) and PTEN inhibitor [bpV(phen)] in LPS−24h (Fig. 20) suggest that the enhanced conversion of PIP_2 into PIP_3 might explain the attenuated I_{Kir} despite the increased plasma membrane localization of Kir2.2.

A variety of ion channels electrostatically interacts with PIP_2, and are either inhibited or activated by PIP_2 availability (D'Avanzo et al., 2010; Hansen et al., 2011; Martin, 2001; Suh et al., 2008). Since the relative amount of PIP_3 is very small among the anionic phospholipids in the plasma membrane (Nasuhoglu et al., 2002), endogenous PIP_3−dependent regulation of ion channel activity is thought to be less likely, although TRPC1 and CNG channels may be the exceptions (Bright et al., 2007; Saleh et al., 2009). However, no previous

study has suggested that PI3K regulates PIP_2-dependent ion channels by altering PIP_2 availability.

We compared these levels using confocal microscopy of THP-1 cells transfected with PH-PLCδ-GFP and PH-Akt-GFP demonstrates the dynamic changes in PIP_2 and PIP_3 levels in LPS-24h, respectively (Fig. 22). Although the anionic charge of PIP_3 is greater than that of PIP_2, its efficiency in Kir2.2 activation is far lower than that of PIP_2 (Rohacs et al., 1999), which might explain the spontaneous decrease in $I_{Kir,LPS}$. In the PIP_2-dependent channel activity, I_{Kir} is detectable in as little as PIP_2, but appear to plateau at over the physiological concentration (D'Avanzo et al., 2010). Besides, PIP_2 on the plasma membrane is dynamically distributed non-uniformly and may be located in raft-like domains (Martin, 2001). Specialized microdomains, or raft, rich in glycosphingolipids and cholesterol within plasma membranes have been reported to concentrate PIP_2, possibly accounting for half of the total PIP_2 at the cell surface (Czech, 2000; Hilgemann, 2007; Jean et al., 2012). Therefore, we do not hesitate to suggest that PIP_2 conversion to PIP_3 by PI3K activation is sufficient to regulate the Kir2.2 activity, although PIP_2 is not completely depleted on the plasma

membrane. And, it would be worth investigating whether similar regulation of PIP_2-dependent ion channels by PI3K occurs in other cell types.

Excessive activation of monocytes/macrophages *in vivo* by a bolus of LPS can lead to septic shock, a serious systemic disorder that can result in multiple organ failure and death. Although cytokines are important for the efficient control of pathogens, overproduction of cytokines can be harmful for the host (Dobrovolskaia et al., 2002), since it may lead to multiple organ failure and death. Activation of the PI3K-Akt pathway via LPS stimulation has been shown to negatively regulate NF-κB activation and the expression of inflammatory genes (Guha et al., 2002). Thus, spontaneous decay of I_{Kir} in the later phases of the LPS/TLR4 response might be an example of a negative feedback mechanism via PI3K-dependent pathway.

In summary, we demonstrate that Kir2.2 is functionally upregulated by LPS stimulation via PKCε-dependent membrane trafficking in human monocytes. Subsequent hyperpolarization enhanced Ca^{2+} influx and cytokine secretion. In addition, spontaneous decay of Kir2.2 currents accounts for the decreased availability of PIP_2 due to PI3K activation (Fig. 23).

Considering its involvement in innate immune responses, Kir2.2 in monocytes could serve as an important regulator for LPS-TLR4 response in immune-physiological system.

REFERENCES

Akita Y. Protein kinase C-ε (PKC-ε): its unique structure and function. *J Biochem.* 2002 Dec; 132:847-852.

Aksoy E, Goldman M, and Willems F. Protein kinase C epsilon: a new target to control inflammation and immune-mediated disorders. *Int J Biochem Cell Biol.* 2004 Feb; 36:183-188.

Bonifacino JS and Glick BS. The mechanisms of vesicle budding and fusion. *Cell.* 2004 Jan; 116:153-166.

Bright SR, Rich ED and Varnum MD. Regulation of human cone cyclic nucleotide-gated channels by endogenous phospholipids and exogenously applied phosphatidylinositol 3,4,5-tirsphosphate. *Mol Pharmacol.* 2007 Jan;71:176-83

Colden-Stanfield M. Clustering of very late antigen-4 integrins modulates K^+ currents to alter Ca^{2+}-mediated monocyte function. *Am J Physiol Cell Physiol.* 2002 Sep; 283:C990-C1000.

Colden-Stanfield M and Gallin EK. Modulation of K^+ currents in monocytes by VCAM-1 and E-selectin on activated human endothelium. *Am J Physiol.* 1998 Jul; 275(Pt 1):C267-277.

Colden-Stanfield M and Scanlon M. VCAM-1-induced inwardly rectifying K^+ current enhances Ca^{2+} entry in human THP-1 monocytes. *Am J Physiol Cell Physiol.* 2000 Aug; 279:C488-494.

Comalada M, Xaus J, Valledor AF, Lopez-Lopez C, Pennington DJ, and Celada A. PKCε is involved in JNK activation that mediates LPS-induced TNF-α, which induces apoptosis in macrophages. *Am J Physiol Cell Physiol.* 2003 Nov; 285:C1235-1245.

Czech MP. PIP2 and PIP3: complex roles at the cell surface. *Cell.* 2000 Mar; 100:603-606.

D'Avanzo N, Cheng WW, Doyle DA, and Nichols CG. Direct and specific activation of human inward rectifier K^+ channels by

membrane phosphatidylinositol 4,5-bisphosphate. *J Biol Chem.* 2010 Nov; 285:37129-37132.

DeCoursey TE, Kim SY, Silver MR, and Quandt FN. Ion channel expression in PMA-differentiated human THP-1 macrophages. *J Membr Biol.* 1996 Jul; 152:141-157.

Dobrovolskaia MA and Vogel SN. Toll receptors, CD14, and macrophage activation and deactivation by LPS. *Microbes Infect.* 2002 Jul; 4:903-914.

Eder C. Regulation of microglial behavior by ion channel activity. *J Neurosci Res.* 2005 Aug; 81:314-321.

Erdogan A, Schaefer CA, Most AK, Schaefer MB, Mayer K, and Tillmanns H et al. Lipopolysaccharide-induced proliferation and adhesion of U937 cells to endothelial cells involves barium chloride sensitive hyperpolarization. *J Endotoxin Res.* 2006; 12:224-230.

Fang Y, Schram G, Romanenko VG, Shi C, Conti L, and Vandenberg CA et al. Functional expression of Kir2.x in human aortic endothelial cells: the dominant role of Kir2.2. *Am J Physiol Cell Physiol.* 2005 Nov; 289:C1134-1144.

Feng Y, Yu S, Lasell TK, Jadhav AP, Macia E, and Chardin P et al. Exo1: a new chemical inhibitor of the exocytic pathway. *Proc Natl Acad Sci U S A.* 2003 May; 100:6469-6474.

Floto RA, Mahaut-Smith MP, Allen JM, and Somasundaram B. Differentiation of the human monocytic cell line U937 results in an upregulation of the calcium release-activated current, ICRAC. *J Physiol.* 1996 Sep; 495(Pt 2):331-338.

Franchini L, Levi G, and Visentin S. Inwardly rectifying K^+ channels influence Ca^{2+} entry due to nucleotide receptor activation in microglia. *Cell Calcium.* 2004 May; 35:449-459.

Gendelman HE, Ding S, Gong N, Liu J, Ramirez SH, and Persidsky Y et al. Monocyte chemotactic protein-1 regulates

voltage-gated K^+ channels and macrophage transmigration. *J Neuroimmune Pharmacol.* 2009 Mar; 4:47-59.

Guha M and Mackman N. LPS induction of gene expression in human monocytes. *Cell Signal.* 2001 Feb; 13:85-94.

Guha M and Mackman N. The phosphatidylinositol 3-kinase-Akt pathway limits lipopolysaccharide activation of signaling pathways and expression of inflammatory mediators in human monocytic cells. *J Biol Chem.* 2002 Aug; 277:32124-32132.

Hansen SB, Tao X, and MacKinnon R. Structural basis of PIP_2 activation of the classical inward rectifier K^+ channel Kir2.2. *Nature.* 2011 Sep; 477:495-498.

Hibino H, Inanobe A, Furutani K, Murakami S, Findlay I, and Kurachi Y. Inwardly rectifying potassium channels: their structure, function, and physiological roles. *Physiol Rev.* 2010 Jan; 90:291-366.

Hilgemann DW. Local PIP_2 signals: when, where, and how? *Pflugers Arch.* 2007 Oct; 455:55-67.

Hinard V, Belin D, Konig S, Bader CR, and Bernheim L. Initiation of human myoblast differentiation via dephosphorylation of Kir2.1 K^+ channels at tyrosine 242. *Development.* 2008 Mar; 135:859-867.

Hirai H, Sootome H, Nakatsuru Y, Miyama K, Taguchi S and Tsujioka K, et al. MK-2206, an allosteric Akt inhibitor, enhances antitumor efficacy by standard chemotherapeutic agents or molecular targeted drugs in vitro and in vivo. *Mol Cancer Ther.* 2010 Jul; 9:1956-1967.

Jansen JA, de Boer TP, Wolswinkel R, van Veen TA, Vos MA and van Rijen HV*, et al.* Lysosome mediated Kir2.1 breakdown directly influences inward rectifier current density. *Biochem Biophys Res Commun.* 2008 Mar; 367:687-692.

Jean S and Kiger AA. Coordination between RAB GTPase and phosphoinositide regulation and functions. *Nat Rev Mol Cell Biol.* 2012 Jul; 13:463-470.

Jo H, Lo PK, Li Y, Loison F, Green S and Wang J, et al. Deactivation of Akt by a small molecule inhibitor targeting pleckstrin homology domain and facilitating Akt ubiquitination. *Proc Natl Acad Sci U S A.* 2011 Apr; 108:6486-6491.

Kim SY, Silver MR, and DeCoursey TE. Ion channels in human THP-1 monocytes. *J Membr Biol.* 1996 Jul; 152:117-130.

Kubo Y, Adelman JP, Clapham DE, Jan LY, Karschin A, and Kurachi Y et al. International Union of Pharmacology. LIV. Nomenclature and molecular relationships of inwardly rectifying potassium channels. *Pharmacol Rev.* 2005 Dec; 57:509-526.

Lan JY, Skeberdis VA, Jover T, Grooms SY, Lin Y, and Araneda RC et al. Protein kinase C modulates NMDA receptor trafficking and gating. *Nat Neurosci.* 2001 Apr; 4:382-390.

Lu YC, Yeh WC and Ohashi PS. LPS/TLR4 signal transduction pathway. *Cytokine.* 2008 May; 42:145-151.

Macia E, Ehrlich M, Massol R, Boucrot E, Brunner C, and Kirchhausen T. Dynasore, a cell-permeable inhibitor of dynamin. *Dev Cell.* 2006 Jun; 10:839-850.

Martin TF. PI(4,5)P_2 regulation of surface membrane traffic. *Curr Opin Cell Biol.* 2001 Aug; 13:493-499.

Muscella A, Marsigliante S, Verri T, Urso L, Dimitri C, and Botta G et al. PKCε-dependent cytosol-to-membrane translocation of pendrin in rat thyroid PC Cl3 cells. *J Cell Physiol.* 2008 Oct; 217:103-112.

Nam JH, Lee HS, Nguyen YH, Kang TM, Lee SW, and Kim HY et al. Mechanosensitive activation of K^+ channel via phospholipase C-induced depletion of phosphatidylinositol 4,5-bisphosphate in B lymphocytes. *J Physiol.* 2007 Aug; 582(Pt 3):977-990.

Nasuhoglu C, Feng S, Mao J, Yamamoto M, Yin HL and Earnest S et al. Nonradioactive analysis of phosphatidylinositeds and other anionic phospholipids by anion-exchange high-performance liquid chromatography with suppressed conductivity detection. *Anal Biochem.* 2002 Feb; 301:243-54.

Okkenhaug K and Vanhaesebroeck B. PI3K in lymphocyte development, differentiation and activation. *Nat Rev Immunol.* 2003 Apr; 3:317-330.

Qin Z. The use of THP-1 cells as a model for mimicking the function and regulation of monocytes and macrophages in the vasculature. *Atherosclerosis.* 2012 Mar; 221:2-11.

Qiu MR, Campbell TJ, and Breit SN. A potassium ion channel is involved in cytokine production by activated human macrophages. *Clin Exp Immunol.* 2002 Oct; 130:67-74.

Ramos AM, Fernandez C, Amran D, Sancho P, de Blas E, and Aller P. Pharmacologic inhibitors of PI3K/Akt potentiate the apoptotic action of the antileukemic drug arsenic trioxide via

glutathione depletion and increased peroxide accumulation in myeloid leukemia cells. *Blood.* 2005 May; 105:4013-4020.

Rittirsch D, Flierl MA and Ward PA. Harmful molecular mechanisms in sepsis. *Nat Rev Immunol.* 2008 Oct; 8:776-787.

Rohacs T, Chen J, Prestwich GD and Logothetis DE. Distinct specificities of inwardly rectifying K^+ channels for phosphoinositides. *J Biol Chem.* 1999 Dec; 274:36065-72.

Schildberger A, Rossmanith E, Eichhorn T, Strassl K and Weber V. Monocytes, peripheral blood mononuclear cells, and THP-1 cells exhibit different cytokine expression patterns following stimulation with lipopolysaccharide. *Mediators Inflamm.* 2013 May; 697972.

Saleh SN, Albert AP and Large WA. Activation of native TRPC1/C5/C6 channels by endothelin-1 is mediated by both PIP_3 and PIP_2 in rabbit coronary artery myocytes. *J Physiol.* 2009 Nov; 587:5361-75.

Schilling T and Eder C. Lysophosphatidylcholine- and MCP-1-induced chemotaxis of monocytes requires potassium channel activity. *Pflugers Arch.* 2009a Nov; 459:71-77.

Schilling T and Eder C. Non-selective cation channel activity is required for lysophosphatidylcholine-induced monocyte migration. *J Cell Physiol.* 2009b Nov; 221:325-334.

Schmid AC, Byrne RD, Vilar R, and Woscholski R. Bisperoxovanadium compounds are potent PTEN inhibitors. *FEBS Lett.* 2004 May; 566:35-38.

Shapira L, Takashiba S, Champagne C, Amar S, and Van Dyke TE. Involvement of protein kinase C and protein tyrosine kinase in lipopolysaccharide-induced TNF-α and IL-1β production by human monocytes. *J Immunol.* 1994 Aug; 153:1818-1824.

Shi C and Pamer EG. Monocyte recruitment during infection and inflammation. *Nat Rev Immunol.* 2011 Oct; 11:762-774.

Steele DF, Eldstrom J, and Fedida D. Mechanisms of cardiac potassium channel trafficking. *J Physiol.* 2007 Jul; 582(Pt 1):17-26.

Suh BC and Hille B. PIP_2 is a necessary cofactor for ion channel function: how and why? *Annu Rev Biophys.* 2008 Mar; 37:175-95.

Tare M, Prestwich SA, Gordienko DV, Parveen S, Carver JE, and Robinson C et al. Inwardly rectifying whole cell potassium current in human blood eosinophils. *J Physiol.* 1998 Jan; 506 (Pt2):303-318.

Tong Y, Brandt GS, Li M, Shapovalov G, Slimko E, and Karschin A et al. Tyrosine decaging leads to substantial membrane trafficking during modulation of an inward rectifier potassium channel. *J Gen Physiol.* 2001 Feb; 117:103-118.

Troutman TD, Bazan JF, and Pasare C. Toll-like receptors, signaling adapters and regulation of the pro-inflammatory response by PI3K. *Cell Cycle.* 2012 Oct; 11:3559-3567.

Vicente R, Escalada A, Coma M, Fuster G, Sanchez-Tillo E, and Lopez-Iglesias C et al. Differential voltage-dependent K^+ channel responses during proliferation and activation in macrophages. *J Biol Chem.* 2003 Nov; 278:46307-46320.

Wang HR, Wu M, Yu H, Long S, Stevens A, and Engers DW et al. Selective inhibition of the $K_{ir}2$ family of inward rectifier potassium channels by a small molecule probe: the discovery, SAR, and pharmacological characterization of ML133. *ACS Chem Biol.* 2011 Aug; 6:845-856.

Way KJ, Chou E, and King GL. Identification of PKC-isoform-specific biological actions using pharmacological approaches. *Trends Pharmacol Sci.* 2000 May; 21:181-187.

Wehrhahn J, Kraft R, Harteneck C, and Hauschildt S. Transient receptor potential melastatin 2 is required for lipopolysaccharide-induced cytokine production in human monocytes. *J Immunol.* 2010 Mar; 184:2386-2393.

Wischmeyer E, Doring F, and Karschin A. Acute suppression of inwardly rectifying Kir2.1 channels by direct tyrosine kinase phosphorylation. *J Biol Chem.* 1998 Dec; 273:34063-34068.

Yin X, Cuello F, Mayr U, Hao Z, Hornshaw M, and Ehler E et al. Proteomics analysis of the cardiac myofilament subproteome reveals dynamic alterations in phosphatase subunit distribution. *Mol Cell Proteomics.* 2010 Mar; 9:497-509.

Young A, Gentzsch M, Abban CY, Jia Y, Meneses PI, and Bridges RJ et al. Dynasore inhibits removal of wild-type and ΔF508 cystic fibrosis transmembrane conductance regulator (CFTR) from the plasma membrane. *Biochem J.* 2009 Aug; 421:377-385.

Zaritsky JJ, Redell JB, Tempel BL, and Schwarz TL. The consequences of disrupting cardiac inwardly rectifying K^+ current (I_{K1}) as revealed by the targeted deletion of the murine Kir2.1 and Kir2.2 genes. *J Physiol.* 2001 Jun; 533(Pt3):697-710.

국문 초록

선천성 면역 (innate immunity)에 관여하는 단핵구 및 대식세포는 여러 수용체 자극에 의해 활성화된다. 그람 (Gram) 음성균의 세포막 구성성분인 지질다당질 (LPS)은 이들 세포에 발현되어 있는 Toll-like 수용체 (TLR4)에 의해 인식되며, 활성화 매개물질로 널리 사용되고 있다. 단핵구의 분화 및 활성화에서 포타슘 이온통로의 변화가 다양함에도 불구하고, 그의 역할 및 기전에 관한 연구는 잘 알려져 있지 않다. LPS 자극한 단핵구에서 전압 의존성 포타슘 이온통로 (Kv)와 칼슘 의존성 포타슘 이온통로 (KCa)의 전도도는 자극 6 시간 이후부터 각각 증가 또는 감소하였다, 뿐만 아니라, LPS 자극 이전에는 거의 관찰되지 않던 내향 정류성 포타슘 이온통로 (Kir)의 전도도는 자극 4 시간에서 최대로 증가하며, 그 이후부터 24 시간까지 자발적으로 감소하는 것을 확인하였다. 따라서, 본 연구에서는 사람 단핵구에서 LPS 자극에 의한 Kir 이온통로의 역할 및 기전을 관찰하였다.

LPS 자극에 의해 증가되는 Kir 전류는 단일 이온통로 전도도 (37.7 pS)와 바륨 (Ba^{2+})에 의한 억제효과 (IC_{50}, 1.42 μM)로 Kir2.2 의 특성임을 알았으며, Kir2.2 의 단백질 발현도 새롭게 확인하였다. THP-1 에서 관찰되는 Kir2.2 는 사람 말초혈액에서 분리한 단핵구에도 존재하며, LPS 자극에 의해서 유사한 Kir

전류변화를 확인하였다. LPS 에 의한 Kir2.2 전류 증가는 세포의 안정막 전위를 과분극시키는 특성에 따라 store-operated Ca^{2+} entry (SOCE)를 증가시키며, TNFα 및 IL-8 과 같은 사이토카인 분비에 관여한다.

LPS 에 의한 Kir2.2 전류 증가는 세포막에서 Kir2.2 이온통로가 증가하는 것으로 보아, 세포막으로의 이동에 의한 것임을 알 수 있었다. 위상차 현미경을 통해 Kir2.2 의 막이동을 확인하였으며, 이러한 현상은 막단백질의 이동을 억제 (Exo-1 과 Brefeldin A)시켜 차단됨을 확인하였다. 또한, Kir2.2 의 막이동은 단백질 인산화효소 C (PKC) 억제제와 siPKCε 에 의해 차단되는 것으로 PKCε 의존적임을 알 수 있었다.

세포막으로 이동하는 Kir2.2 는 계속 증가함에도 불구하고, 4 시간 이후부터는 Kir 전도도가 자발적으로 감소하였다. LPS/TLR4 자극 신호는 PI3K 를 활성화 시키며, 이는 PIP_2 를 PIP_3 로 전환하여 Akt/PKB 경로를 활성화한다. 이때 감소하는 PIP_2 에 의해 Kir2.2 의 활성도가 조절 받는 것으로 생각된다. 자발적으로 감소하는 Kir 전류는 PI3K 억제제 (LY294002 와 wortmannin)에 의해 다시 회복되며, Akt 억제제는 어떠한 영향을 미치지 않는 것으로 보아, 직접적인 PIP_2 감소가 Kir2.2 전류 감소를 유발하는 것을 알 수 있다.

본 연구를 요약하면, 사람 단핵구에서 LPS 자극에 의한 Kir 전도도의 증감현상은 Kir2.2 의 PKCε 의존적인 세포막 이동과 PI3K 활성화에 의한 PIP_2 감소가 복합적으로 일어나는 현상임을 알 수 있다. 또한, Kir2.2 전류의 변화는 세포막 전위의 과분극을 일으켜 세포 내 Ca^{2+} 유입 및 사이토카인 분비를 조절하는 것으로 보인다. 이는 박테리아 등의 감염에 의한 선천성 면역반응에서 단핵구의 중요한 생리학적 역할을 이해하는데 크게 기여할 수 있을 것이다.

주요어 : 단핵구, 지질다당질, Kir2.2, THP-1, PIP_2, PI3K

학 번 : 2010-21899